Tz=-1 → 0 β-Decays of 54Ni, 50Fe, 46Cr, and 42Ti and Comparison With Mirror (3He,t) Measurements

Molina, F.; Rubio, B.; Fujita, Y.; Gelletly, W.; Agramunt, J.; Algora, A.; Benlliure, J.; Boutachkov, P.; Cáceres, L.; Cakirli, R. B.; Casarejos, E.; Domingo-Pardo, C.; Doornenbal, P.; Gadea, A.; Ganioğlu, E.; Gascón, M.; Geissel, H.; Gerl, J.; Górska, M.; Grbosz, J.; Hoischen, Robert; Kumar, R.; Kurz, N.; Kojouharov, I.; Susam, L. Amon; Matsubara, H.; Morales, A. I.; Oktem, Y.; Pauwels, D.; Pérez-Loureiro, D.; Pietri, S.; Podolyák, Zs.; Prokopowicz, W.; Rudolph, Dirk; Schaffner, H.; Steer, S. J.; Tain, J. L.; Tamii, A.; Tashenov, S.; Valiente-Dobón, J. J.; Verma, S.; Wollersheim, H-J.

Published in:
Physical Review C (Nuclear Physics)

DOI:
10.1103/PhysRevC.91.014301

2015

$T_z = -1 \rightarrow 0$ β decays of ^{54}Ni, ^{50}Fe, ^{46}Cr, and ^{42}Ti and comparison with mirror (^{3}He,t) measurements

F. Molina,[1,*] B. Rubio,[1,†] Y. Fujita,[2,3] W. Gelletly,[4] J. Agramunt,[1] A. Algora,[1,5] J. Benlliure,[6] P. Boutachkov,[7] L. Cáceres,[7,8] R. B. Cakirli,[9] E. Casarejos,[6,‡] C. Domingo-Pardo,[1,10] P. Doornenbal,[7] A. Gadea,[1,11] E. Ganioğlu,[9] M. Gascón,[6,§] H. Geissel,[7] J. Gerl,[7] M. Górska,[7] J. Gręboszc,[7,12] R. Hoischen,[7,13] R. Kumar,[14] N. Kurz,[7] I. Kojouharov,[7] L. Amon Susam,[9] H. Matsubara,[3,‖] A. I. Morales,[6] Y. Oktem,[9] D. Pauwels,[15] D. Pérez-Loureiro,[6] S. Pietri,[4] Zs. Podolyák,[4] W. Prokopowicz,[7] D. Rudolph,[13] H. Schaffner,[7] S. J. Steer,[4] J. L. Tain,[1] A. Tamii,[3] S. Tashenov,[7] J. J. Valiente-Dobón,[11] S. Verma,[6] and H-J. Wollersheim[7]

[1]*Instituto de Física Corpuscular, CSIC-Universidad de Valencia, E-46071 Valencia, Spain*
[2]*Department of Physics, Osaka University, Toyonaka, Osaka 560-0043, Japan*
[3]*Research Center for Nuclear Physics, Osaka University, Ibaraki, Osaka 567-0047, Japan*
[4]*Department of Physics, University of Surrey, Guildford GU2 7XH, Surrey, United Kingdom*
[5]*Institute of Nuclear Research (ATOMKI), H-4001 Debrecen, P.O. Box 51, Hungary*
[6]*Universidad de Santiago de Compostela, E-15782 Santiago de Compostela, Spain*
[7]*Gesellschaft für Schwerionenforschung, Planckstrasse 1, D-64291 Darmstadt, Germany*
[8]*Universidad Autónoma de Madrid, E-28049 Madrid, Spain*
[9]*Department of Physics, Istanbul University, Istanbul 34134, Turkey*
[10]*Forschungszentrum Karlsruhe, D-76344 Eggenstein-Leopoldshafen, Germany*
[11]*INFN-Laboratorio Nazionale di Legnaro, I-35020 Legnaro (PD), Italy*
[12]*The Henryk Niewodniczanski Institute of Nuclear Physics, (IFJ PAN), Kraków, Poland*
[13]*Department of Physics, Lund University, S-22100 Lund, Sweden*
[14]*Inter University Accelerator Centre, Post Box No. 10502, New Delhi 110067, India*
[15]*Instituut voor Kern- en Stralingsfysica, K.U. Leuven, B-3001 Leuven, Belgium*

(Received 24 June 2014; revised manuscript received 18 October 2014; published 5 January 2015)

We have studied the β decay of the $T_z = -1$, $f_{7/2}$ shell nuclei ^{54}Ni, ^{50}Fe, ^{46}Cr, and ^{42}Ti produced in fragmentation reactions. The proton separation energies in the daughter $T_z = 0$ nuclei are relatively large (≈4–5 MeV) so studies of the γ rays are essential. The experiments were performed at GSI as part of the Stopped-beam campaign with the RISING setup consisting of 15 Euroball Cluster Ge detectors. From the newly obtained high precision β-decay half-lives, excitation energies, and β branching ratios, we were able to extract Fermi and Gamow-Teller transition strengths in these β decays. With these improved results it was possible to compare in detail the Gamow-Teller (GT) transition strengths observed in beta decay including a sensitivity limit with the strengths of the $T_z = +1$ to $T_z = 0$ transitions derived from high resolution (^{3}He,t) reactions on the mirror target nuclei at RCNP, Osaka. The accumulated B(GT) strength obtained from both experiments looks very similar although the charge exchange reaction provides information on a broader energy range. Using the "merged analysis" one can obtain a full picture of the B(GT) over the full Q_β range. Looking at the individual transitions some differences are observed, especially for the weak transitions. Their possible origins are discussed.

DOI: 10.1103/PhysRevC.91.014301 PACS number(s): 23.40.Hc, 21.10.Hw, 23.20.Lv, 25.55.Kr

I. INTRODUCTION

The determination of accurate Gamow-Teller (GT) transition strengths, B(GT) values, is very important in the study of nuclear structure and nuclear astrophysics. This is because they are intimately related to the overlap between the wave functions of the initial and final states involved in the transformation. The operator is the well-understood operator $\sigma\tau$. Hence the B(GT) values derived from experiments can be used to test nuclear structure models and also act as a guide to calculate B(GT) values and the associated half-lives ($T_{1/2}$) of exotic β-decaying nuclei that are experimentally inaccessible at present.

Gamow-Teller transitions can be studied in two different ways, namely in β decay mediated by the weak interaction, and in charge exchange (CE) reactions where the strong interaction is involved [1]. The β decay has the advantage of providing absolute B(GT) values, the GT transition strengths, but is limited by the energy window available. In contrast, CE reactions provide only relative B(GT) values at present, but there are no restrictions on the accessible excitation energy in the final nucleus. Ideally one would like to perform both β decay and CE reactions on the same nucleus leading to the same final nucleus and compare the results. This would provide a comparison of the two probes and determine whether they give similar results. However, the CE experiment, which would

*Present address: Comisión Chilena de Energía Nuclear, P.O. Box 188-D, Santiago, Chile.
†berta.rubio@ific.uv.es
‡Present address: Universidad de Vigo, E-36310 Vigo, Spain.
§Present address: Lawrence Berkeley National Laboratory, Berkeley, CA, USA.
‖Present address: National Institute of Radiological Sciences (NIRS), Chiba 263-8555, Japan.

involve intense beams of radioactive, exotic nuclei and a highly demanding experimental setup is not yet feasible although it is firmly on the agenda for several future facilities; see, for instance, [2]. An alternative approach is to assume isospin symmetry and to compare β decay and CE reactions in mirror nuclei. Assuming the same GT response in mirror transitions, one can combine them to produce a complete picture of the GT strengths as a function of excitation energy for the two mass A isobars. This is possible when a stable target is available for the appropriate CE study. The transitions from $T_z = \pm 1$ nuclei to the same final $T_z = 0$ nucleus, among the possible mirror combinations, is the simplest because we need only assume isospin symmetry for the initial two nuclei. With this idea in mind, we have launched a series of experiments at GSI (Helmholtzzentrum für Schwerionenforschung), where we have studied the complete set of β decays of the even-even $T_z = -1$, $f_{7/2}$-shell nuclei ^{54}Ni, ^{50}Fe, ^{46}Cr, and ^{42}Ti. The results will be compared with the corresponding CE reactions on the $T_z = +1$, stable target nuclei ^{54}Fe, ^{50}Cr, ^{46}Ti, and ^{42}Ca studied at RCNP, Osaka [3–6].

To deduce a B(GT) value for each state fed by a β decay in the daughter nucleus, one has to use the following expression [1],

$$B(\mathrm{GT})^{\beta} = \frac{K}{\lambda^2}\frac{I_\beta(E)}{f(Q_\beta - E, Z)T_{1/2}} = \frac{K}{\lambda^2}\frac{1}{ft}, \qquad (1)$$

where E is the excitation energy of a level in the final nucleus, $I_\beta(E)$ is the β feeding to the level, $f(Q_\beta - E, Z)$ is the value of the Fermi function for the energy $(Q_\beta - E)$ and a daughter nucleus of atomic number Z, $T_{1/2}$ is the parent β half-life, $K = 6143.6(17)$ [7], and $\lambda = g_A/g_V = -1.270(3)$ [8]. Thus, we need the following observables: the β feeding, the $T_{1/2}$, and the Q_β value. In the β-decay study of ^{54}Ni, ^{50}Fe, ^{46}Cr, and ^{42}Ti, we have measured the first two of these quantities, while the Q_β values were taken from Ref. [9].

II. EXPERIMENTAL DETAILS

The β-decay experiments were performed as part of the stopped-beam RISING campaign at GSI. The nuclei ^{54}Ni, ^{50}Fe, ^{46}Cr, and ^{42}Ti were produced by the fragmentation of a ^{58}Ni beam at 680 MeV/nucleon on a 400 mg/cm^2 Be target in separate runs optimized to transport and implant the nucleus of interest. The SIS-18 synchrotron [10] delivered the ^{58}Ni primary beam with a spill structure of 10 s ON and 3 s OFF and an intensity of 2×10^9 particles per spill. The reaction fragments were separated in-flight in the fragment separator (FRS) [see Fig. 1(a)] [11,12]. The nuclei traversing the FRS were identified according to the atomic charge (which in the present case was equal to Z, i.e., the nuclei were fully stripped) and the mass-over-charge ratio A/Q. The charge of the fully stripped ions was determined from the energy loss registered in twomultisampling ionization chambers (MUSICs) located at the end of the spectrometer.

The A/Q value was determined using the magnetic rigidity and the velocity of the fragments. The magnetic rigidity was calculated using the magnetic fields and the positions of the fragments at the intermediate image plane (S2) using the scintillator SC21 and the final image plane (S4) using the multiwire proportional counters MW41 and MW42. The velocity of the fragments was derived from the time of flight measured using the time signals provided by SCI21 and SCI41 and the position of the fragments. The resulting identification plot for all the ions arriving at SCI41 in the ^{54}Ni run is shown in Fig. 2 as an example.

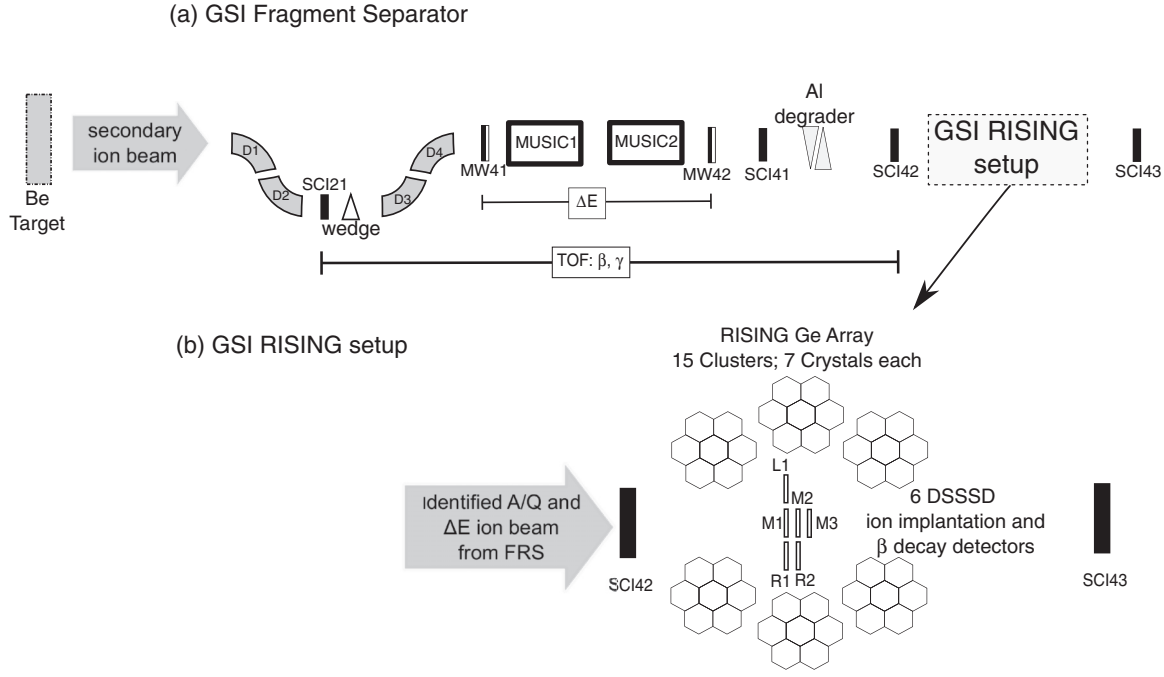

FIG. 1. The schematic layout of the FRS separator and the various detectors used for the identification of the ions. In the lower part of the figure, a schematic layout of the RISING setup including the arrangement of the six DSSSDs is shown.

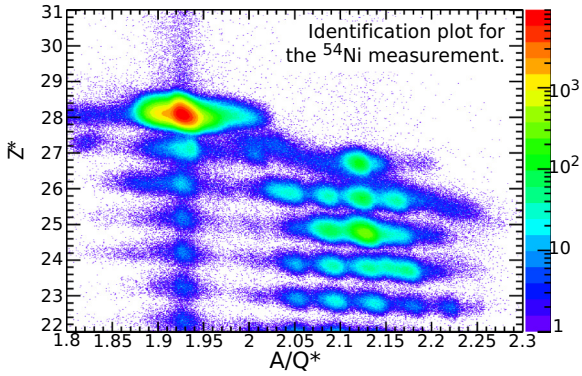

FIG. 2. (Color online) Identification plot for the reaction fragments separated and identified up to SCI41 in the ^{54}Ni run. Z^* and A/Q^* are adjusted to give the correct Z and A/Q for ^{54}Ni. Small differences from the correct Z and A/Q may exist for the other nuclear species.

The separated ions were implanted in one of the six double-sided silicon strip detectors (DSSSDs), each with 16 X and 16 Y strips defining 256 pixels, and a size of $50 \times 50 \times 1$ mm^3 forming an array [13] arranged as shown in Fig. 1(b). The FRS was operated in achromatic mode. Although the ions of interest dominated at the final focal plane, several other ion species survived the separation process and were implanted in the implantation detectors. To improve the sensitivity of selection further, an aluminium energy degrader, placed before the DSSSD, was adjusted so that most of the desired ions were implanted in the DSSSD M2. Therefore, the off-line analysis was performed for the events in which the implantations occurred in the M2 detector (see later for the conditions for implanted ions). This also helped us to obtain accurate efficiencies for the γ detectors because the position of the implanted ions was well defined.

In Fig. 3(a), we present the same identification plot as shown in Fig. 2 with the additional condition that the implantation occurred in M2. As the figure shows the ^{54}Ni ions implanted in M2 (3.9×10^6 counts during the full run) can be clearly separated from the rest of the ions (1.8×10^6). Figures 3(b)–3(d) show the identification plots with the condition that the implants occurred in M2 for ^{50}Fe, ^{46}Cr, and ^{42}Ti. The β particles also deposit energy in the same DSSSDs and they provided the β-decay signals. A logarithmic amplifier was used to amplify the energy signals produced by the β particles (few hundreds of keV) and the energy signals produced by the implants (few tens of GeV) (see Figs. 4 and 5). Two kinds of trigger were used in the present experiment: an implantation signal (SCI41 and DSSSD) or a decay signal (only a DSSSD). Typical counting rates were ~0.5 implantations/pixel/s and ~0.6 decays/pixel/s in M2 for the ^{54}Ni run. Similar counting rates were obtained in the other cases. The distinction between the two triggers allows a software correlation analysis between the implant and the decay demanding that the two signals occurred in the same pixel of the DSSSD.

As we see in Fig. 1(b), the implantation setup was surrounded by the RISING γ-ray array [14] consisting of 15 Euroball Cluster Ge detectors [15] in a 4π geometry. They were distributed in three rings of five Clusters each, at 51°,

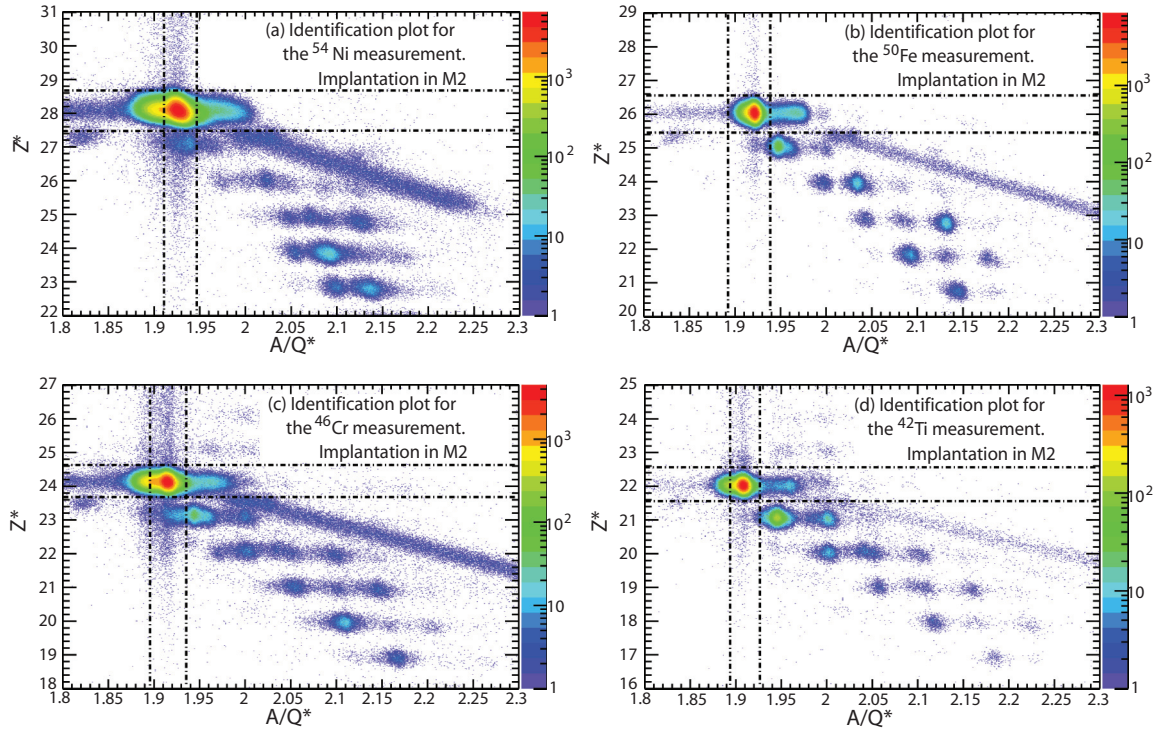

FIG. 3. (Color online) Identification plots of the reaction fragments separated and identified, including the implantation condition in detector M2, for the four measurements. The window to select the desired implant is shown for each case. Z^* and A/Q^* are the correct Z and A/Q for the desired nuclei in each case; small differences from the correct Z and A/Q may exist for the other nuclear species.

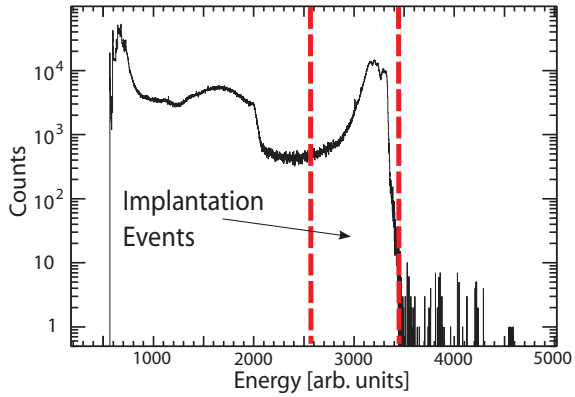

FIG. 4. (Color online) Sum of all aligned but not calibrated M2 DSSSD Y-Strip signals for implantation events in the ^{54}Ni measurement. The vertical lines show the selected implantation energy range in arbitrary units (a.u.).

90°, and 129° with respect to the beam axis. The distance from the front face of the Ge detectors to the middle position of the M2 active stopper was approximately 22 cm (see latter). Each Cluster consists of seven hexagonal Ge crystals. In this experiment, measurements of the intensities of γ rays were essential to deduce the feeding to excited states in the daughter nucleus. Some of these states were expected to lie at high excitation energy. Consequently, an array with high efficiency, such as the RISING array was essential with an accurate efficiency calibration up to high energy. Therefore, a particular effort was dedicated to calibrating the efficiency of the array. After the experiment, the detector M2 was removed and replaced by a dummy detector with a pointlike source in the center. ^{152}Eu, ^{60}Co, ^{137}Cs, and ^{226}Ra radioactive sources were used for the efficiency calibration up to 2.5 MeV and Monte Carlo simulations for energies up to 6 MeV as described in Sec. III B (cf. Fig. 6). The efficiency was 17.1(6)% at 0.662 MeV and 11.9(4)% at 1.173 MeV. The energy calibration was done before, during, and after the experiment.

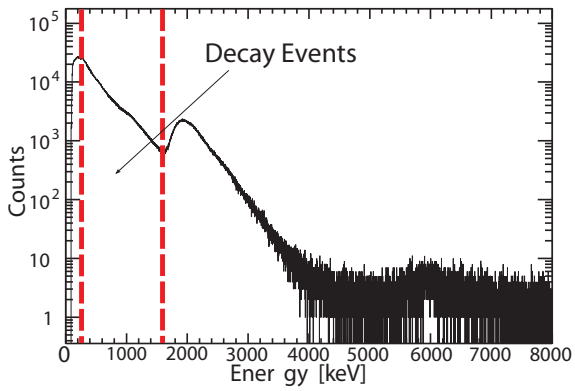

FIG. 5. (Color online) Sum of all aligned but not calibrated M2 DSSSD Y-Strip signals for decay events in the ^{54}Ni measurement. The red lines (color online) show the selected β-decay energy range.

III. ANALYSIS AND RESULTS

A. Half-life analysis

The β-decay half-life $T_{1/2}$ is essential if we are to extract B(GT) values. Previous $T_{1/2}$ values for the decay of ^{54}Ni, ^{50}Fe, ^{46}Cr, and ^{42}Ti are reported in Refs. [17–21] (see Table I). However, except for ^{42}Ti, the desired accuracy of less than a few percent had not been achieved.

To deduce the $T_{1/2}$ values, we used time correlations between signals from the heavy-ion implantation (defining $t = 0$) and the β decay that happened in the same pixel of the M2 DSSSD with the condition for A/Q and Z for the nucleus of interest set as shown in Fig. 3.

As mentioned above, the counting rates were relatively high. Therefore, it was expected that there are large numbers of randomly correlated events and that some events from real correlations are not properly collected, if the simple consecutive implantation-decay events were correlated. To ensure that all real correlations are included in the analysis, we correlated each β-decay event with all the implantations that happened in the period ±5 s before and after the decay event. As a result we have all the true correlations as well as a large number of events from random correlations. The latter have to be subtracted. The background subtraction was delicate, because of the time structure of the primary beam which influences the time structure of the random correlations. The oscillating structure of the background is clearly seen in Fig. 7. The 13-s period of the background is related to the 10 s ON and 3 s OFF spill structure of the primary beam from the SIS18 synchrotron. The background was determined by constructing a "wrong" correlation spectrum in which every decay that happened in pixel (i, j) was correlated with all the implants that happened in pixel (j, i) (where $i \neq j$). A detailed explanation of the method is given in Ref. [22]. The spectra obtained after the subtraction of the "wrong" correlations are shown in Fig. 8 for all four cases.

It can be seen that the resulting background is flat and the counts are close to zero (see Table II fourth column). By selecting the nucleus of interest from the implantation events, we ensure that only this specific nucleus contributes as the parent activity, and we assume that the daughter activity is produced as a decay product. Therefore, each decay curve was fitted with two components, i.e., the decay of the $T_z = -1$ parent activity, and the growth and decay of the $T_z = 0$ daughter activity. Because the $T_z = 0$ daughter nuclei make the so-called superallowed decays, their half-lives are well studied [7,21]. They were thus fixed in the fit. In Fig. 8 and in column three of Table I, we present the $T_{1/2}$ values obtained by using the least squares fit minimization method. Maximum likelihood fits gave very similar results.

Correlations between the implants and the β-γ events were also constructed for the lowest 1^+ to 0^+ γ transition in the four cases. The statistics were reduced because of the efficiency of the γ array, but there is the corresponding advantage that only the parent decay is involved in the fit. The results of these fits are also presented in Table I. The uncertainties are larger but the numbers are fully consistent with the implant-β correlation analysis. Overall the accuracy of the $T_{1/2}$ values was improved by one to two orders of magnitude for the decays of ^{54}Ni, ^{50}Fe, and ^{46}Cr (see Table I, third column).

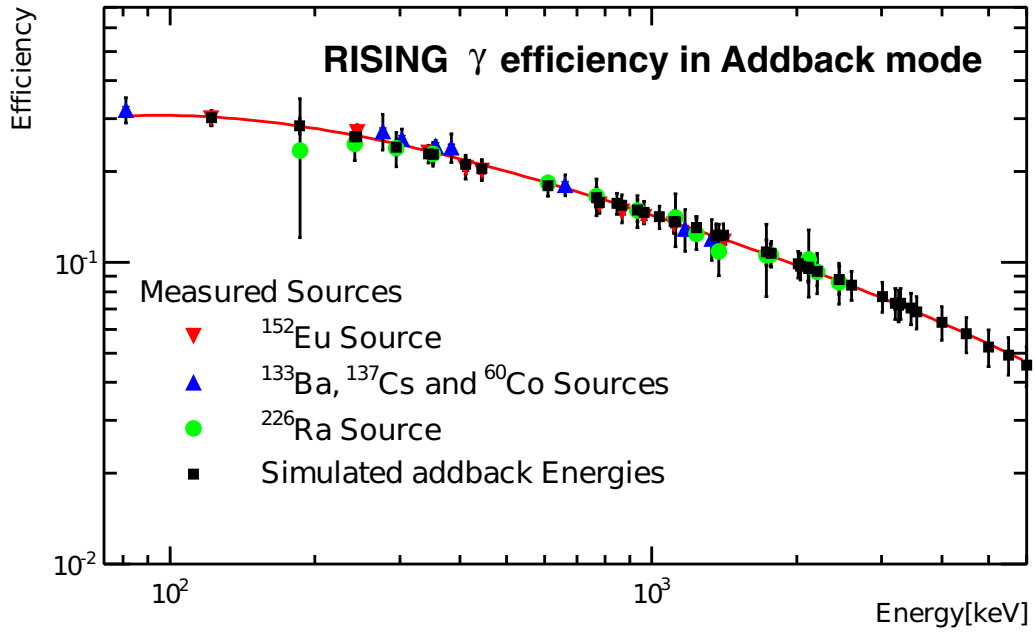

FIG. 6. (Color online) Experimental and simulated γ efficiencies using add-back. The experimental values for ^{60}Co, ^{133}Ba, ^{137}Cs, ^{152}Eu, and ^{226}Ra are shown as triangles and circles. The simulated efficiencies are shown as squares. Both experimental and simulated values were fitted using $\ln[\epsilon(E_\gamma)] = \sum_{k=0}^{5} p_k(\ln(E_\gamma)^k$ [16], where $\epsilon(E_\gamma)$ is the γ efficiency at energy E_γ and p_k values are the fitting parameters for the RISING Ge array [$p_0 = 50.31(4)$, $p_1 = -43.38(1)$, $p_2 = 14.42(1)$, $p_3 = -2.350(1)$, $p_4 = 18.74(1)\times10^{-2}$, and $p_6 = -58.84(3)\times10^{-4}$]. The resulting efficiency curve is shown by the solid line.

B. Gamma analysis and level schemes

As described above, efficiency and energy calibrations of the γ-ray detectors were carried out using standard sources of known absolute strengths up to the excitation energy of 2.4 MeV (see Fig. 6). Extended Monte Carlo simulations using GEANT4 [23] were carried out to determine the efficiency beyond the last calibration point. In the simulations the nominal distance between the sources and the front surfaces of the Cluster detectors was adjusted to 23 cm to reproduce the experimental points. The simulations showed that the difference between a "pointlike" source and an extended source illuminating the full M2 detector was negligible in comparison with other uncertainties. Moreover, the reliability of our efficiency calibration was further confirmed by the observation of the three γ rays with energies 436.8(1), 1227.8(1), and 1524.9(2) keV observed in the ^{42}Ti setting (Fig. 12). They belong to the decay of the 62.0 s 7^+ isomer in ^{42}Sc [24] and have almost equal intensities. The results of the simulations were confirmed using a ^{56}Co source (covering a range from 0.8 to 3.5 MeV) with the same setup some months after the experiment.

Each Cluster was used in add-back mode, namely, the energy deposited in any two neighboring crystals within a 100-ns time interval was added together (see the spectra in Figs. 9–12). A typical add-back improvement factor over the single-crystal

TABLE I. The β-decay half-lives of ^{54}Ni, ^{50}Fe, ^{46}Cr, and ^{42}Ti. The literature values are from Refs. [17–21]

Parent Nucleus	$T_{1/2}$ (ms) literature	$T_{1/2}$(ms) Present work β analysis	$T_{1/2}$(ms) Present work γ analysis
^{54}Ni	111(7)	114.2(3)	114.3(18)
^{50}Fe	155(11)	152.1(6)	150.1(29)
^{46}Cr	240(140)	224.3(13)	223.9(99)
^{42}Ti	208.14(45)	211.7(19)	209.5(52)

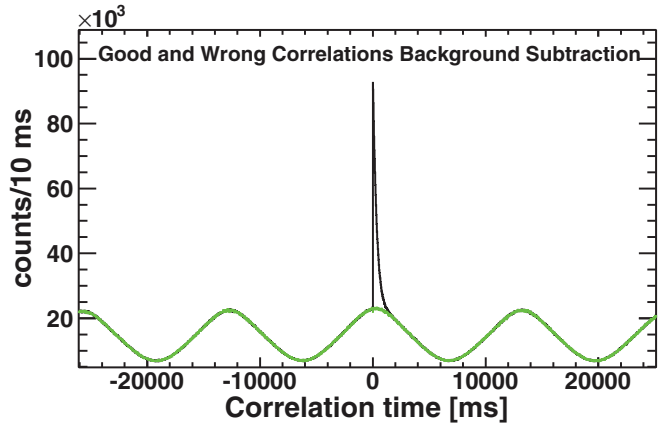

FIG. 7. (Color online) "Good correlations" (in black) between beta and implantation events happening in the same pixel (i, j) as a function of correlation time. "Wrong correlations" (in green) between beta events happening in pixel (i, j), and implantations happening in the opposite pixel (j,i) (for $i \neq j$). The "Wrong correlation" background was normalized to the "Good correlations" data. As can be seen in the figure both spectra overlap perfectly. The 13-s period of the oscillating background is related to the 10 s ON and 3 s OFF spill structure of the primary beam from the SIS18 synchrotron.

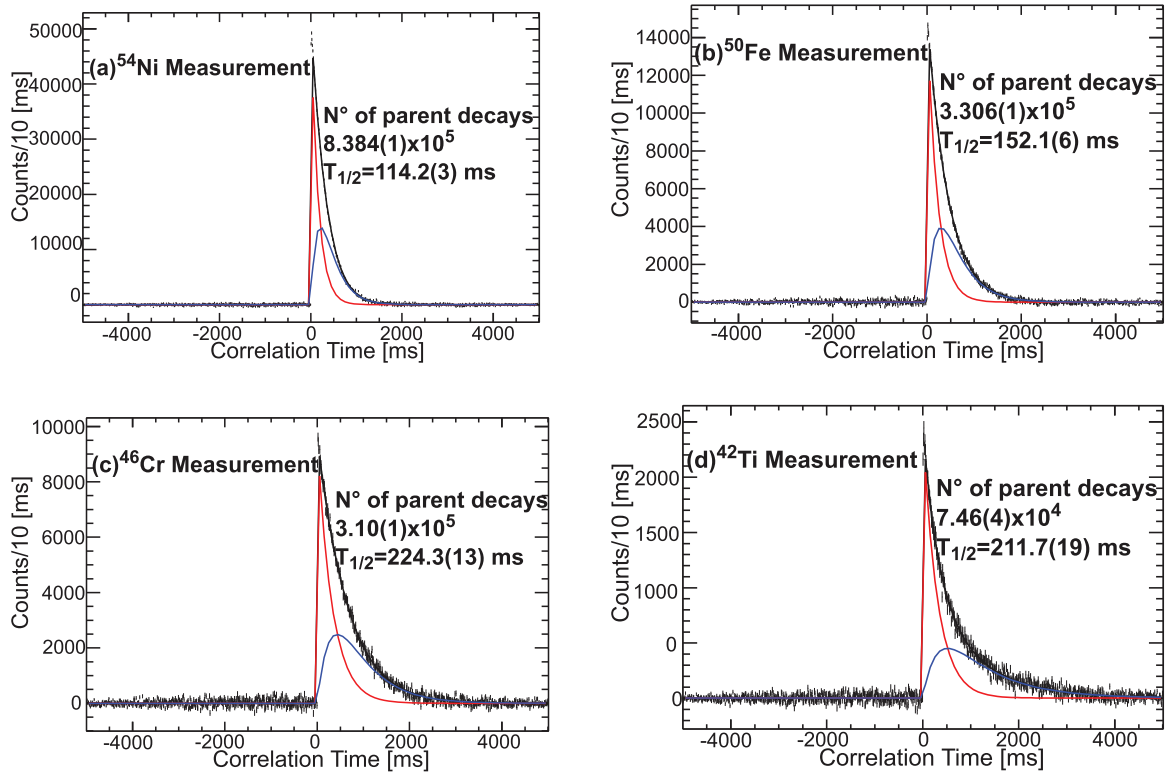

FIG. 8. (Color online) The figure shows the implantation-β correlations for (a) ^{54}Ni, (b) ^{50}Fe, (c) ^{46}Cr, and (d) ^{42}Ti with the background from the random correlations subtracted (see text for details). The fits to the decay curves obtained were made with two components namely the decay of initial $T_z = -1$ nuclei and the growth and decay of $T_z = 0$ daughter nuclei. As a result the half-lives of the $T_z = -1$ nuclei were obtained (see text).

analysis was 30% for 1-MeV and 60% for 3-MeV γ rays. The energy calibration and gain matching of the detectors were carried out for each individual crystal every few runs to check for possible electronic shifts before applying the add-back. The energy calibration was linear and extrapolated to high energies. The accuracy of the calibration could be examined with the known energies of several γ rays observed in different runs. For example, the known 5523.1(12)-keV line in ^{44}Ti [25] was observed at 5522.6(4) keV in our experiment [see Fig. 11(f)].

The full γ-decay spectra in add-back mode in prompt coincidence (250 ns) with the β signals in the M2 detector, but without any condition on the implanted nuclei, are shown in Figs. 9–12 for the measurements of ^{54}Ni, ^{50}Fe, ^{46}Cr, and ^{42}Ti, respectively. As expected from the particle identification plot shown in Fig. 3, the γ peaks in the $T_z = 0$ daughter nuclei ^{54}Co, ^{50}Mn, ^{46}V, and ^{42}Sc are prominent and the well-known γ transitions from the first 1^+ states to the 0^+, ground states are the most intense lines in all of these spectra. Some other γ lines are also visible. They belong either to the nucleus of interest or to other fragments reaching the M2 detector. Their origins are indicated in each of the figures. It should be noted that in the $T_{1/2}$ analysis explained earlier a condition was set on the nucleus of interest. Consequently these contaminant γ lines had a negligible effect.

TABLE II. List of important parameters after fitting the beta-implantation correlations as shown in Fig. 8.

Parent nucleus	Parent half-life $T_{1/2}$ (ms)	Number of decaying parents N_β^0	Constant background after subtraction
^{54}Ni	114.2(3)	838406(1163)	0.79(471)
^{50}Fe	152.1(6)	330631(691)	−2.25(221)
^{46}Cr	224.3(13)	310120(1016)	0.78(316)
^{42}Ti	211.7(19)	74624(368)	2.72(96)

To identify previously unidentified γ lines in the $T_z = 0$ daughter nuclei, we used the information from the corresponding CE reactions. The four (^{3}He,t) reactions on mirror $T_z = +1$ target nuclei ^{54}Fe, ^{50}Cr, ^{46}Ti, and ^{42}Ca were performed with a high energy resolution of ∼30 keV at RCNP, Osaka [3–6] using the Grand Raiden spectrometer. In these reactions, the 1^+ states populated by the GT transitions were identified. In our delayed-γ-ray measurements, we expect to see the γ rays from these 1^+ states to the 0^+ ground state or to other excited states. It should be noted that all the 1^+ states observed in the CE reactions which were expected within the sensitivity limits of the present experiments were identified through the observation of 1^+ to 0^+ γ transitions. In addition, transitions from the excited 1^+ states to the first 2^+ states were observed in two cases. This was confirmed by γ-γ coincidences. No other candidates for γ transitions from the β decay of these nuclei were found in the spectra. The decay schemes deduced are presented in Figs. 13–16.

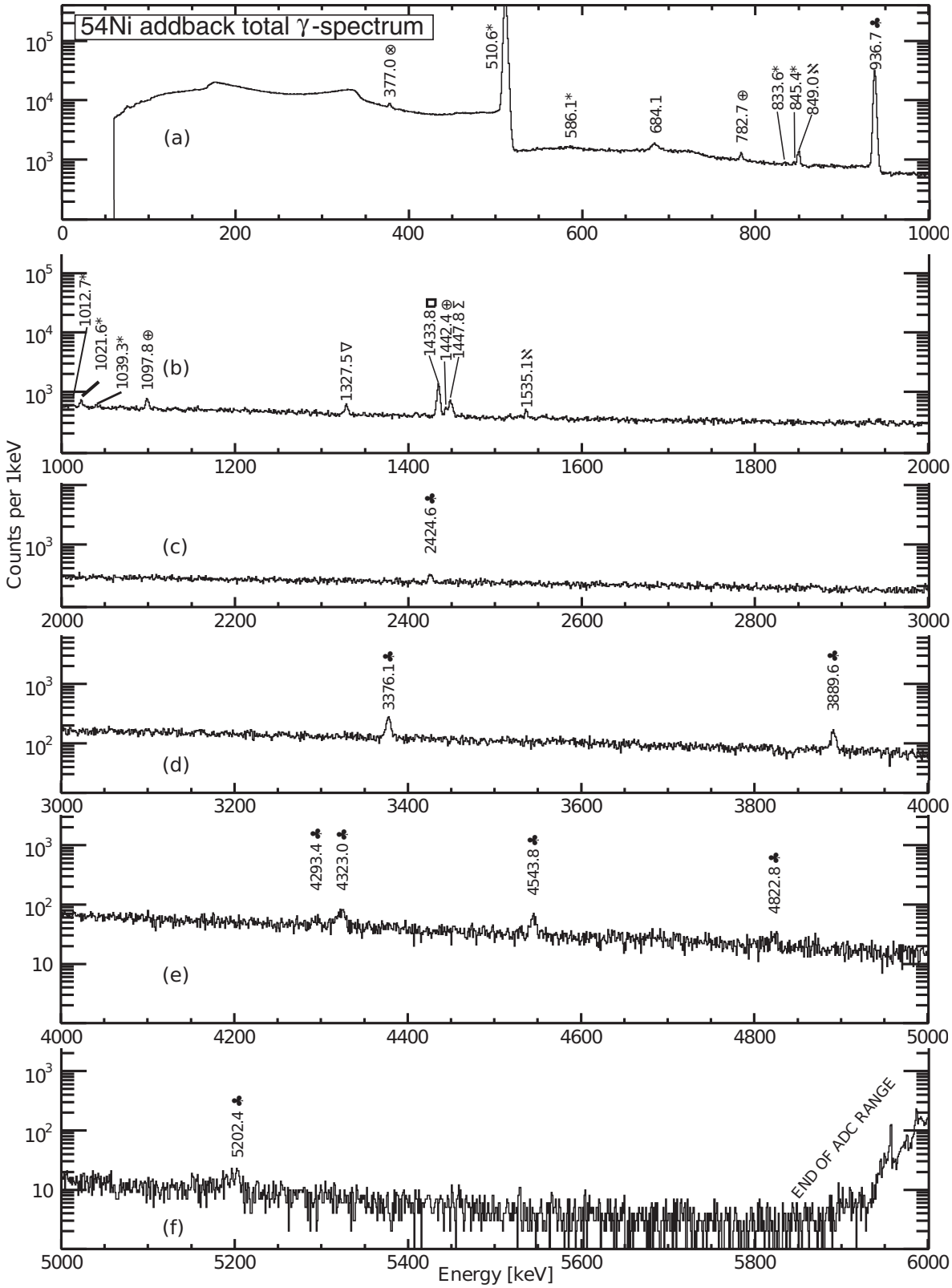

FIG. 9. The γ spectrum obtained in the add-back mode for the ^{54}Ni FRS setting in coincidence with β particles, but without any condition on the implanted nuclei. The identified γ lines in the ^{54}Co daughter nucleus from the decay of the ^{54}Ni mother nucleus are marked with the symbol ♣. Gamma lines in the spectrum are also identified that correspond to neutron capture in Ge and Al (*), the summing of two gammas (Σ), and γ rays from the decay of other nuclei implanted in the M2 DSSSD such as ^{53}Mn ($\otimes$, from ^{53}Fe β^+ decay [26]), ^{50}Cr ($\oplus$, from ^{50}Mn β^+ decay [27]), ^{52}Fe ($\aleph$, from ^{52}Co β^+ decay [28] or ^{53}Co p decay [29]), ^{53}Fe (∇, from ^{53}Co β^+ decay [30]), and ^{52}Cr ($\square$, from ^{52m}Mn β^+ decay [31]).

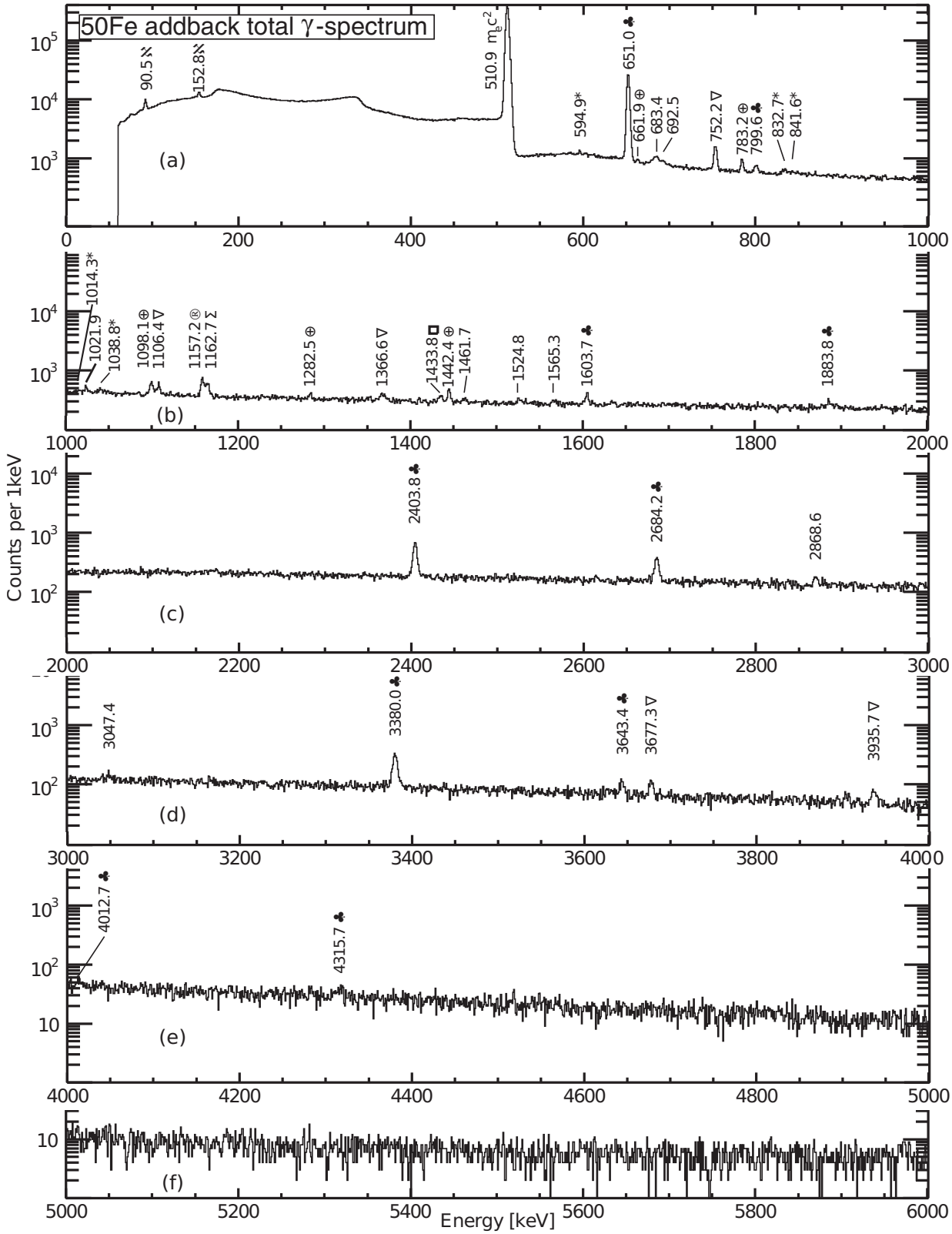

FIG. 10. The γ spectrum obtained in the add-back mode for the ^{50}Fe FRS setting in coincidence with β particles, but without any condition on the implanted nuclei. The identified γ lines in the ^{50}Mn daughter nucleus from the decay of the ^{50}Fe mother nucleus are marked with the symbol ♣. Gamma lines in the spectra are also identified that correspond to neutron capture in Ge and Al (*), the summing of two gammas (Σ), and γ rays from the decay of other nuclei implanted in the M2 DSSSD such as ^{49}V (ℵ, from ^{49}Cr β^+ decay [32]), ^{50}Cr ($\oplus$, from ^{50m}Mn β^+ decay [27]), ^{48}Cr (∇, from ^{48}Mn β^+ decay [33]), ^{44}Ca (®, from ^{44}Sc β^+ decay [34]), and ^{52}Cr (□, from ^{52m}Mn β^+ decay [31]).

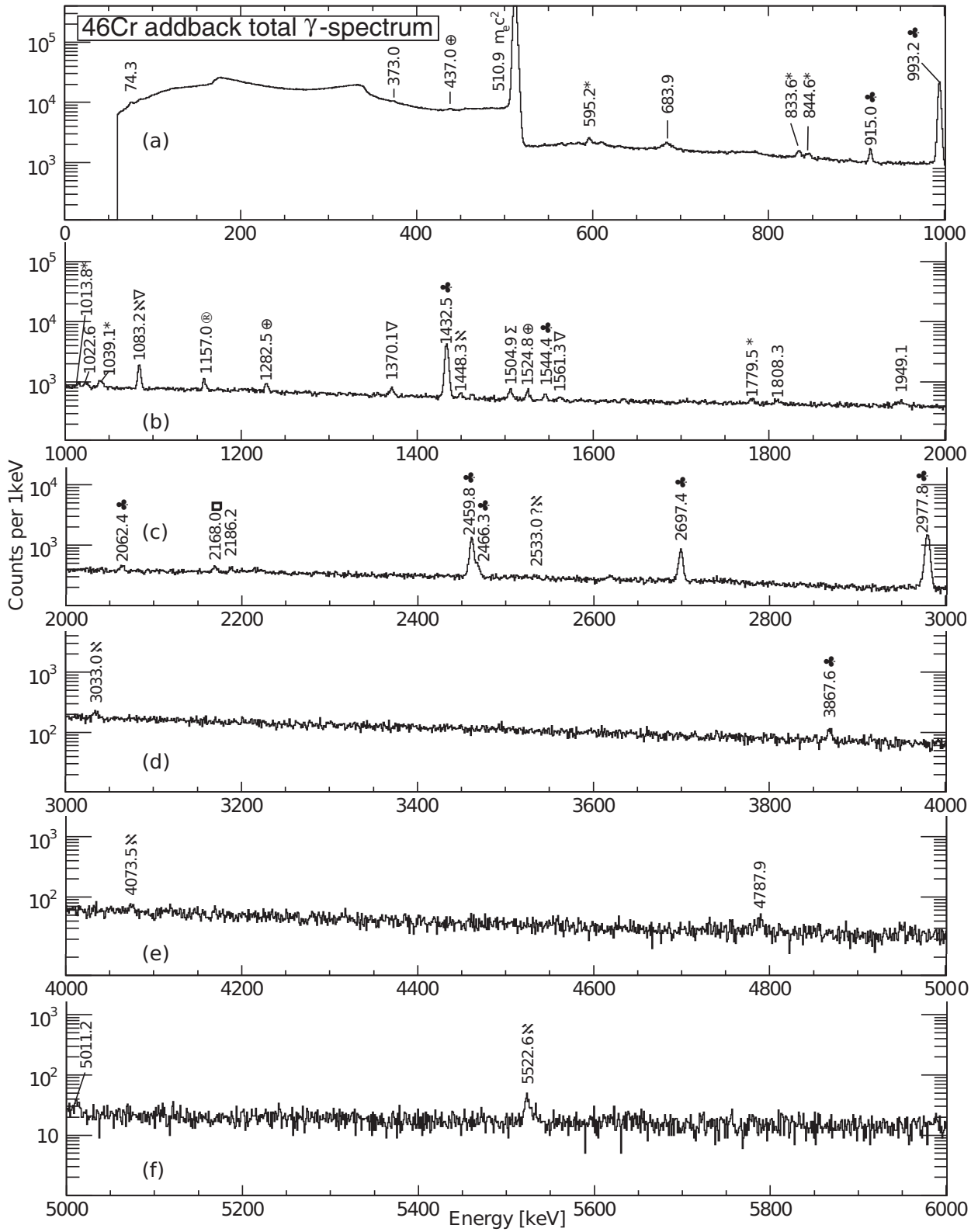

FIG. 11. The γ spectrum obtained in the add-back mode for the ^{46}Cr FRS setting in coincidence with β particles, but without any condition on the implanted nuclei. The identified γ lines in the ^{46}V daughter nucleus from the decay of the ^{46}Cr mother nucleus are marked with the symbol ♣. Gamma lines in the spectra are also identified that correspond to neutron capture in Ge, Al, and Si (*), the summing of two gammas (Σ), and γ rays from the decay of other nuclei implanted in the M2 DSSSD such as ^{42}Ca ($\oplus$, from ^{42m}Sc β^+ decay [35] and ^{42g}Sc β^+ decay [37]), ^{44}Ti (ℵ, from ^{44g}V β^+ decay [28] or ∇ from ^{44m}V β^+ decay [28]), ^{44}Ca(®, from ^{44}Sc β^+ decay [34]), and ^{38}Ar (□, from ^{38}K β^+ decay [38]).

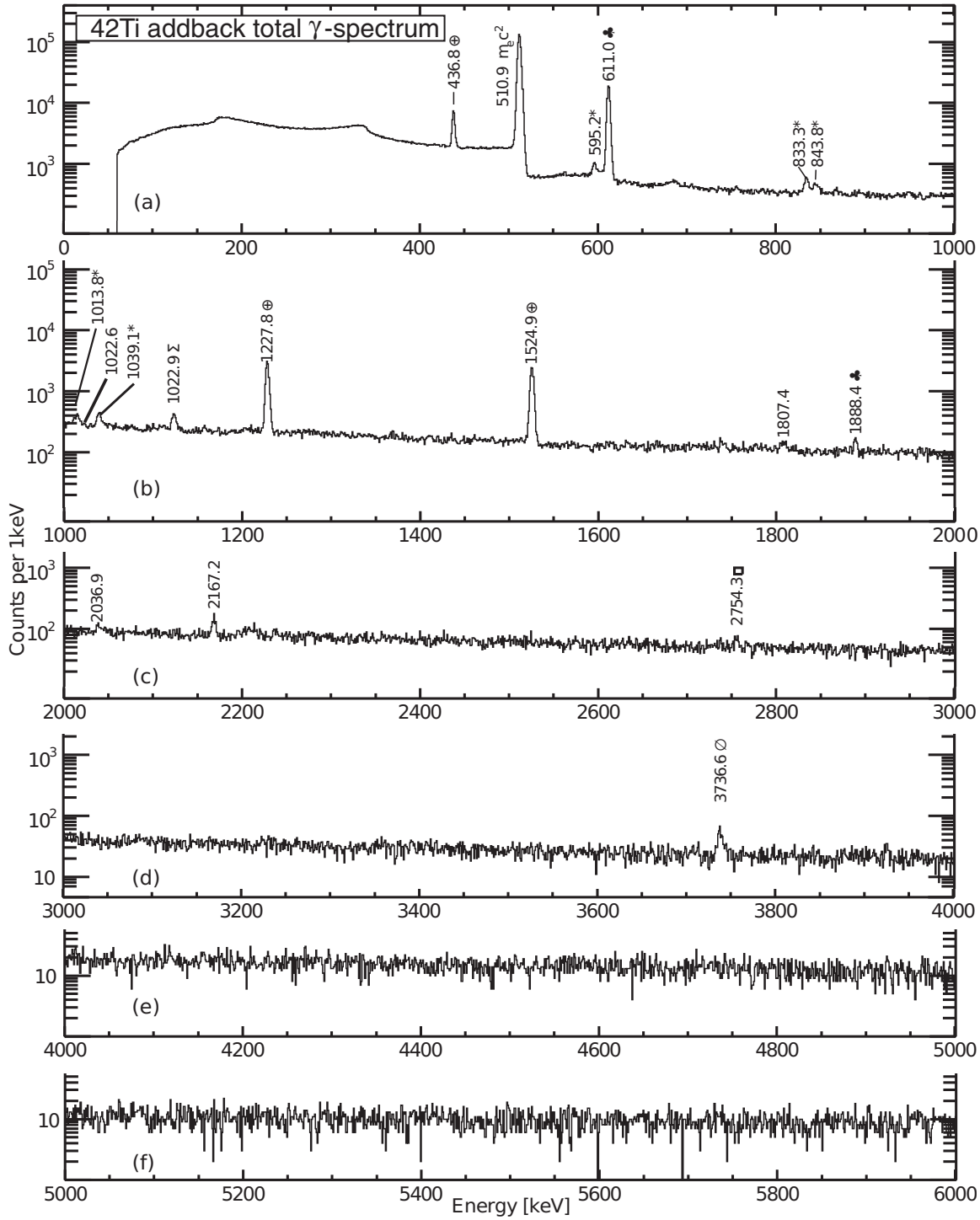

FIG. 12. The γ spectrum obtained in the add-back mode for the ^{42}Ti FRS setting in coincidence with β particles, but without any condition on the implanted nuclei. The identified γ lines in the ^{42}Sc daughter nucleus from the decay of the ^{42}Ti mother nucleus are marked with the symbol ♣. Gamma lines in the spectra are also identified that correspond to neutron capture in Ge and Al (*), the summing of two gammas (Σ), and γ rays from the decay of other nuclei implanted in the DSSSD such as ^{42}Ca ($\oplus$, from ^{42m}Sc β^+ decay [35]), ^{38}Ar ($\square$, from ^{38}K β^+ decay [38]), and ^{40}Ca($\oslash$, from ^{40}Sc β^+ decay).

C. Ground-state feeding, absolute feeding to excited states, and *B*(GT) values

It is not easy to measure the ground-state–to–ground-state feeding in β decay, because there is no γ decay to identify such events. The amount of feeding can be obtained by knowing the number of β-decaying implanted nuclei and subtracting all the feeding to the excited states using the information on the β-delayed γ transitions. However, the precise determination of

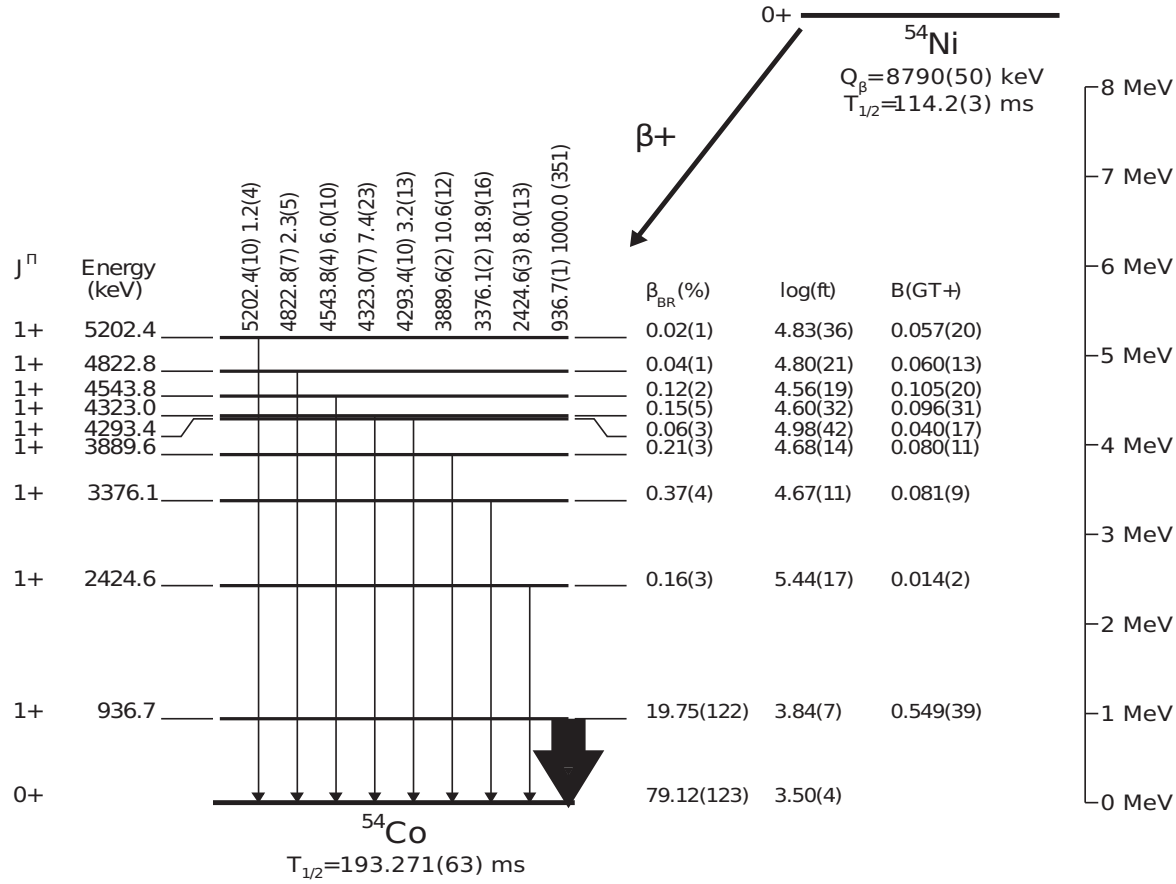

FIG. 13. ^{54}Ni β-decay scheme. All the values given in this figure originate from the present work except for the Q_β value which is taken from [9] and the daughter half-life, taken from [7].

the total number of implantations of the decaying nuclei is also difficult, because the ions are identified only up to SCI41 and not beyond. We can never be sure whether the nuclei remain the same when they are finally implanted in M2 (the fraction which remains the same is called the survival probability). A second difficulty arises from the fact that the γ rays are recorded only if the β decay occurs and is detected. Thus the recording of the γ rays depends on the β-detection efficiency, which is also a difficult quantity to determine precisely.

To illustrate our solution to this problem we will use the ^{54}Ni decay as an example. We want to use the total number of parent β-decay events registered as a normalization. Again, this quantity is not a trivial matter to determine. We know that after an implantation has occurred the subsequent β registered can be from the correct associated β decay, or to the subsequent decay, or to some other random β decay. In consequence we will use the time correlations and the decay fit to retrieve the real number of parent decays.

We know how many ^{54}Ni parent nuclei identified up to SCI41 were implanted in M2 and gave a β-decay signal in the same pixel of the detector consistent with the ^{54}Ni$T_{1/2}$ (see Sec. III A). This number comes out as one of the parameters in the fitting procedure shown in Fig. 8(a). On the other hand, we can make the same kind of time correlation but demand in addition a coincidence between the β particle and the 937-keV γ ray emitted in the decay of the first 1^+ state in ^{54}Co (see Fig. 13). The fit is shown in Fig. 17. Again the number of initial nuclei giving a β-γ signal comes out as a fitting parameter. Thus, the number of 937-keV γ rays emitted per ^{54}Ni decay can be obtained from

$$I^\gamma(937\ \text{keV}) = \frac{N^0(937)}{N^0_\beta \times \epsilon^\gamma(937)}, \tag{2}$$

where $N^0(937)$ is the total number of γ events in the implant-β-γ correlation fit, N^0_β is the total number of β events in the implant-β correlation fit, and ϵ^γ (937) is the γ efficiency at 937 keV.

Once we obtain the absolute intensity for this particular γ ray, the remaining lines can be normalized to its intensity. The absolute feeding to each individual state can then be calculated from the difference in the γ intensity feeding and de-exciting each level. The intensities deduced are given in Tables III–VI. Finally, the ground-state–to–ground-state feeding can then be deduced by subtracting all the feeding to the excited states (see Fig. 13).

A similar procedure was followed in the other three cases. The resulting numbers for the β feeding in percent are given on the right-hand side of each of the level schemes shown in Figs. 13–16. Combining these values with the $T_{1/2}$ values obtained in this experiment and Ref. [21] for ^{42}Ti, and the Fermi function f calculated using the Q values from [9],

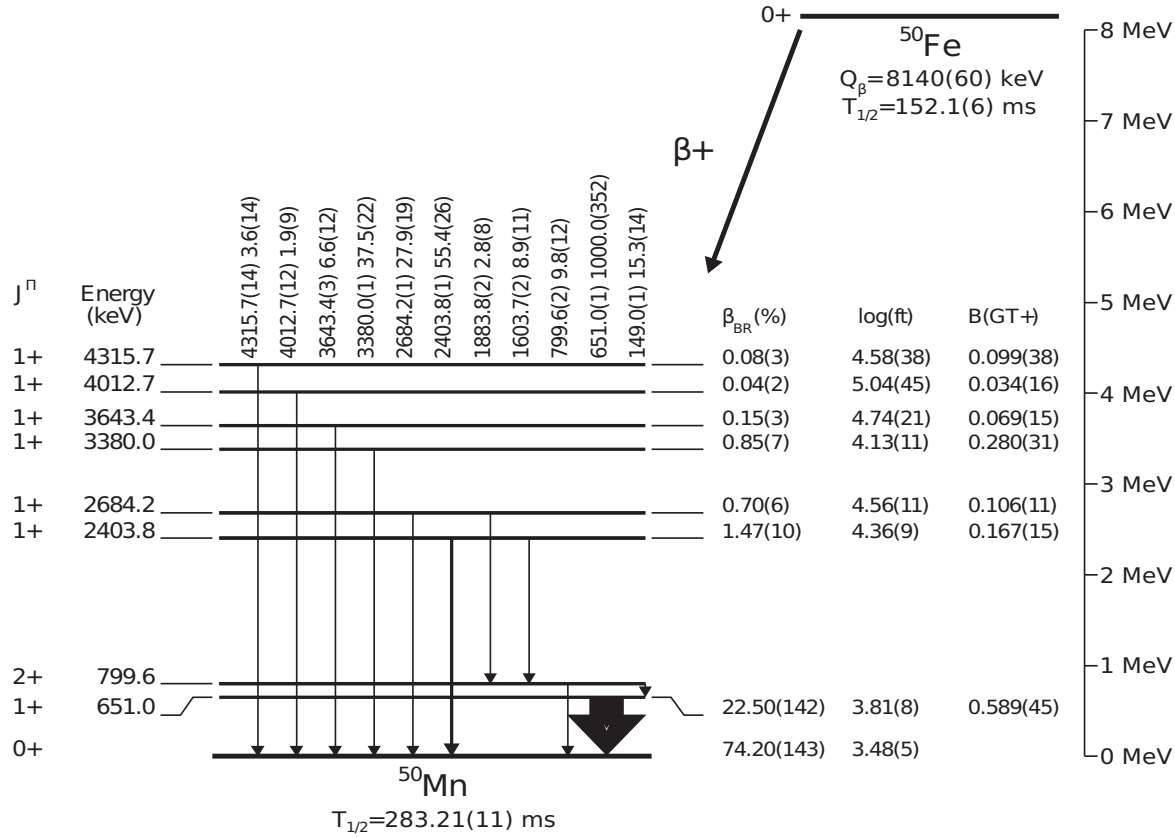

FIG. 14. ^{50}Fe β-decay scheme. All the values given in this figure originate from the present work except for the Q_β value which is taken from [9] and the daughter half-life, taken from [7].

we obtained the $\log ft$ values, which are also shown in these figures. Finally the B(GT) values for the Gamow-Teller transitions [Eq. (1)] populated in the four β decays are shown in the last column in Figs. 13–16 and also in Tables VII–X.

It is worth noting that our measurements of the ground-state–to–ground-state (the IAS) branching ratios, together with the measured ($T_{1/2}$) values and Q values from the literature, allow the determination of the strength of the *superallowed* Fermi transitions between analogue states. As emphasised by Hardy and Towner [36], measurements of transition rates between analogue states provide the most precise value of V_{ud}, the up-down quark mixing element of the Cabibbo-Kobayashi-Maskawa (CKM) matrix which in turn provides an important test of the properties of the electroweak interaction and possible physics beyond the standard model. This matrix element is of paramount importance because it is the major contribution to the unitary test of the CKM matrix,

$$|V_{ud}|^2 + |V_{us}|^2 + |V_{ub}|^2 = 0.99990 \pm 0.00060,$$

where $|V_{ud}|^2 = 0.97425 \pm 0.00022$.

At regular intervals over the last 40 years, Hardy and Towner have published surveys of the information available on *superallowed* Fermi transitions with the latest appearing in 2009 [7]. In general they use odd-odd $T_z = 0$ decays for their calculations. However, in this last survey they listed in addition eight measurements of $T_z = -1$ to $T_z = 0$ β decays including the decay of ^{42}Ti but not ^{46}Cr, ^{50}Fe, and ^{54}Ni because the experimental knowledge for these three decays was not sufficient. Here we provide experimental information for these three cases and improve the knowledge of ^{42}Ti (see below). This extends the systematics for $T_z = -1$ to $T_z = 0$ cases to higher masses. Hopefully this information will be useful in the next evaluation. Our measured $T_{1/2}$ values are given in Table I. The corresponding values for percentage feeding to the ground state are 79.1(12), 74.2 (14), and 77.2 (10) for the ^{54}Ni, ^{50}Fe, and ^{46}Cr decays, respectively.

As mentioned above ^{42}Ti is one of the cases included in the survey of Ref. [7]. The experimental information was revisited by Kurtukian *et al.* in Ref. [21]. They made an effort to extract a very accurate value for the intensity of the 611-keV, 1^+ to $0^+\gamma$ transition. However, in their estimate of the branching to higher excited states they followed the reasoning of Hardy and Towner [7] based on the information in Ref. [37]. In Ref. [37], they claim an intensity for the 2223-keV γ ray that is incompatible with the fact that we did not see this γ-ray line in our data. Moreover this transition was not included in the latest evaluation of the data for ^{42}Ti decay [24] because in the compiler's opinion this line could be contaminated by the ^{1}H(n,γ) background line. Instead we observed the 1888.4-keV line (see Table VI and Fig. 16), with an intensity of 0.41(6)%, that was also seen by Honkanen *et al.* in Ref. [39]. Therefore the ratio $\gamma_{\text{total}}/\gamma_{611} = 0.023$, as reported in Ref. [7] should be changed to 0.007(1) which will make the ground-state–to–ground-state β branching 48.5 (12)

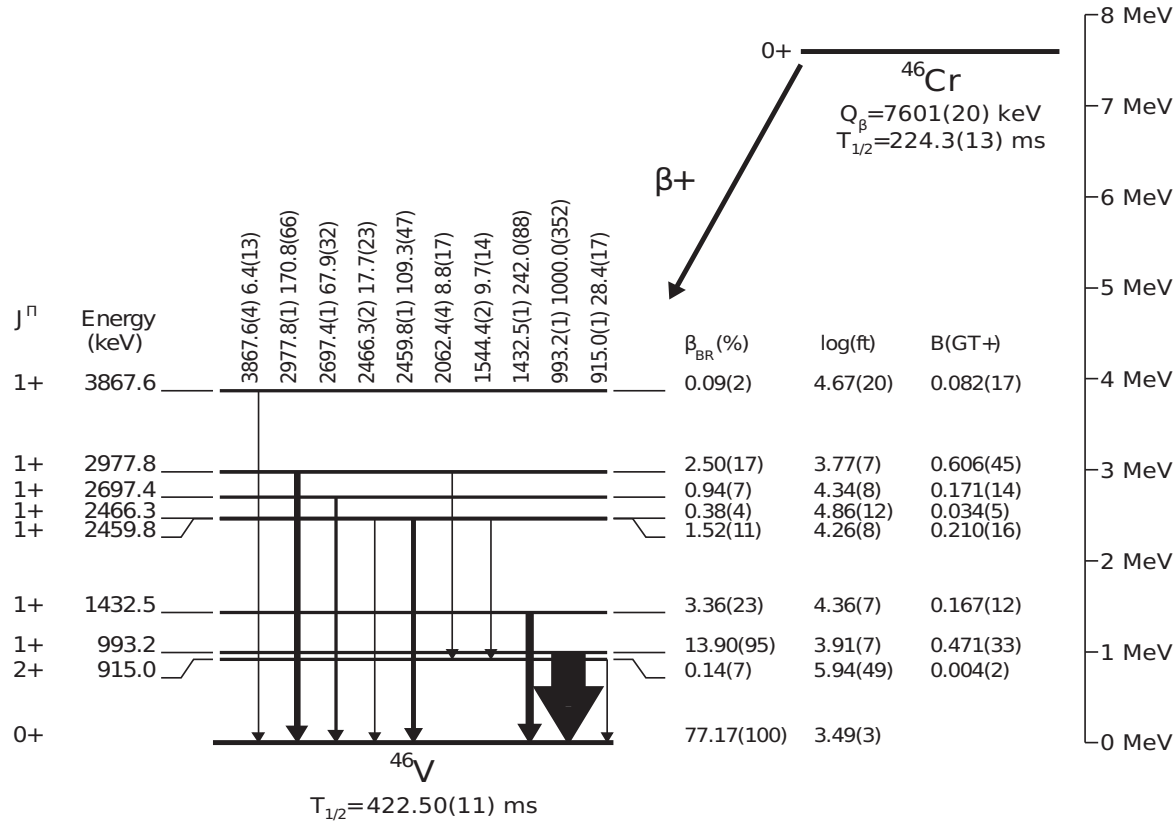

FIG. 15. ^{46}Cr β-decay scheme. All the values given in this figure originate from the present work except for the Q_β value which is taken from [9] and the daughter half-life, taken from [7].

if we use the more precise value of Ref. [21] for the intensity of the 611-keV line. This value is consistent with our less precise value of 43.7(36).

IV. DISCUSSION

A. The γ decay of the $J^\pi = 1^+$ states in $N = Z$ nuclei

In all of the cases studied here we found that the γ transitions from the excited 1^+ states that were populated to the 0^+ ground state were strong. On the other hand, the γ transitions to the $J^\pi = 1^+$ states at lower energies were strongly suppressed, although they can be connected by $M1$ γ transitions. This is consistent with the fact that these $\Delta T = 0$ transitions are expected to be strongly suppressed in $T_z = 0$ nuclei as explained in detail in Ref. [40]. A short note on this particular aspect of this work is in preparation.

B. Mirror Gamow-Teller transitions from β decays and charge-exchange reactions

The main purpose of this paper was to compare β decay and CE reactions and to test the idea of using the merged analysis in cases where the β decay is poorly known. We remind the reader that for the merged analysis the only necessary information from the β decay is the $T_{1/2}$ and the Q_β value. In Sec. III we described our β-decay experiments and how we obtained B(GT) values. In the following we discuss the CE experiments briefly and continue with the comparison of the results coming from both CE and β decay, including the sensitivity limit for the latter.

CE reactions measured at 0° and at intermediate energies of more than 100 MeV per nucleon allow the study of the relative GT transition strengths with no restriction on the energy window because of the close proportionality between the GT cross sections and the B(GT) values [1,41,42],

$$\sigma_j^{\mathrm{GT}}(q,\omega) \simeq \hat{\sigma}^{\mathrm{GT}} F(q,\omega) B_j(\mathrm{GT}), \tag{3}$$

where q is the momentum transfer and ω is the total energy transfer. The value $\hat{\sigma}^{\mathrm{GT}}$ is the unit cross section for the GT transition at $q = \omega = 0$ and a given incoming energy for a system with mass number A. The value $F(q,\omega)$ gives the dependence of the GT cross sections on the momentum and energy transferred. It has a value of unity at $q = \omega = 0$ and usually decreases gradually as a function of excitation energy [43].

At RCNP, Osaka, dispersion matching techniques were applied between a magnetic spectrometer and a beam line system [44,45], and energy resolutions of ~30 keV or even better were achieved in the (p,n)-type CE reaction $(^3\mathrm{He},t)$ at 140 MeV/nucleon and 0°. This resolution is essential if we are going to make a detailed comparison level by level with the β-decay results.

From the CE experiments we derive relative B(GT) values. To determine absolute B(GT) values for all of the GT transitions observed in CE reactions up to high excitation energies, a method called "merged analysis" was proposed

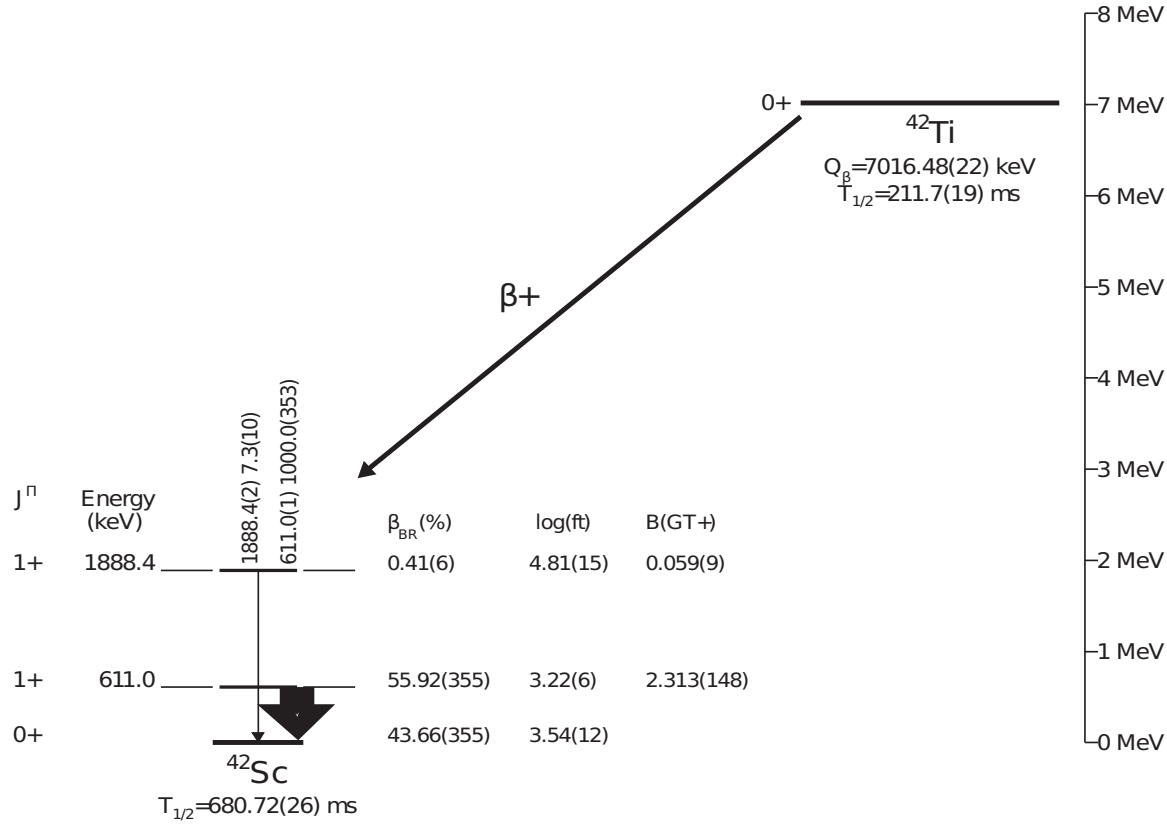

FIG. 16. ^{42}Ti β-decay scheme. All the values given in this figure originate from the present work except for the Q_β value which is taken from [21] and the daughter half-life, taken from [7].

[4] and it is described as follows. The idea is to use the $T_{1/2}$ and Q_β values from the β decay of $T_z = -1, -2\ldots$ nuclei and the relative B(GT) values from CE reactions on the mirror $T_z = +1, +2\ldots$ target nuclei to obtain the absolute B(GT) values. The method is based on two important and nontrivial assumptions, namely that (i) isospin mirror symmetry works, and (ii) we can select only Gamow-Teller transitions in the analysis of the CE reaction cross sections.

The "merged analysis" starts with the formula connecting the total β-decay half-life and the partial half-life t_F of the Fermi transition and t_js of GT transitions,

$$(1/T_{1/2}) = (1/t_F) + \sum_{j=\mathrm{GT}} (1/t_j). \tag{4}$$

The inverse of the half-life represents the transition strength. Therefore, in this formula we assume that the total β-decay strength given on the left side is the sum of the strengths of the Fermi and GT transitions, and that the contribution from

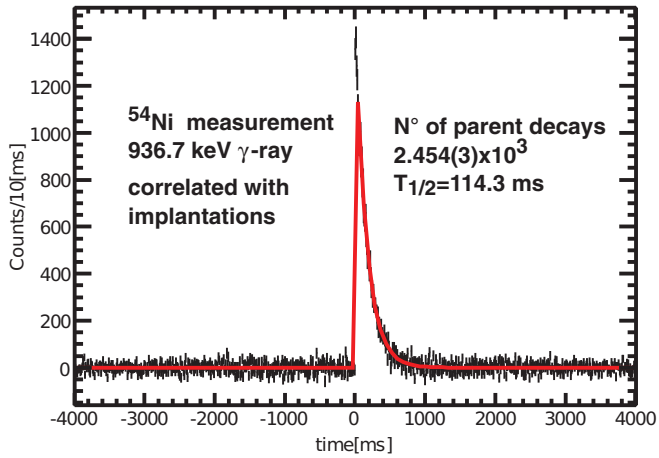

FIG. 17. (Color online) The figure shows the implantation β-γ correlations for ^{54}Ni implants and the 937-keV γ line, with the background of the random correlations subtracted. The fit to the decay curve was made with a single decay component.

TABLE III. List of γ-ray energies and intensities obtained in add-back mode for the decay of ^{54}Ni to ^{54}Co.

Energy (keV)	Counts	$I(\gamma)$
936.7 (1)	104471 (341)	1000.00 (3515)
2424.6 (3)	492 (76)	8.00 (126)
3376.1 (2)	940 (74)	18.85 (161)
3889.6 (2)	481 (53)	10.60 (123)
4293.4 (10)	136 (55)	3.21 (130)
4323.0 (7)	312 (96)	7.42 (230)
4543.8 (4)	245 (40)	6.04 (102)
4822.8 (7)	88 (17)	2.26 (45)
5202.4 (10)	43 (14)	1.18 (38)

TABLE IV. List of γ-ray energies and intensities obtained in add-back mode for the decay of ^{50}Fe to ^{50}Mn.

Energy (keV)	Counts	$I(\gamma)$
149.0 (1)	2415 (221)	15.30 (1380)
651.0 (1)	95382 (333)	1000.00 (3517)
799.6 (2)	849 (100)	9.84 (121)
1603.7 (2)	531 (66)	8.91 (114)
1883.8 (2)	153 (44)	2.81 (81)
2403.8 (1)	2607 (83)	55.37 (262)
2684.2 (1)	1226 (71)	27.86 (188)
3380.0 (1)	1422 (69)	37.45 (223)
3643.4 (3)	240 (41)	6.62 (116)
4012.7 (12)	66 (30)	1.95 (90)
4315.7 (14)	114 (46)	3.56 (142)

forbidden transitions can be neglected. Applying the relationships $B_j(\mathrm{GT})\lambda^2 = K/f_j t_j$ and $B(\mathrm{F})(1-\delta_c) = K/f_\mathrm{F} t_\mathrm{F}$ for the GT and Fermi transition strengths, respectively, one can eliminate both t_F and t_j, and we obtain

$$\frac{1}{T_{1/2}} = \frac{1}{K}\left[B(\mathrm{F})(1-\delta_c)f_\mathrm{F} + \sum_{j=\mathrm{GT}} \lambda^2 B_j(\mathrm{GT}) f_j\right], \quad (5)$$

where f_F and f_j can be calculated if the decay energy is known, $B(\mathrm{F}) = |N-Z|$, and the relative strengths proportional to $B_j(\mathrm{GT})$ can be studied in the (^{3}He,t) reaction [see Eq. (3)]. Therefore, if the total half-life $T_{1/2}$ and Q_β values of the β decay are known accurately, the relative strengths of the $B_j(\mathrm{GT})$ studied in the (^{3}He,t) reaction can be converted into absolute values. One of the main objectives of the present work is to determine the extent to which the assumptions (i) and (ii) mentioned above are fulfilled for $T_z = \pm 1 \rightarrow 0$ GT transitions in the $f_{7/2}$ shell nuclei. Because the accuracies of the $T_{1/2}$ values were considerably improved in the present β-decay measurements, we noticed that better accuracies are achieved for the (^{3}He,t) B(GT) values by renormalizing the literature values using the "merged analysis" described above. For the decay of ^{54}Ni, ^{50}Fe, and ^{46}Cr, we used $T_{1/2}$ values from the present analyses, and for the decay of ^{42}Ti, an even more accurate $T_{1/2}$ value of 209.14(45) ms from Ref. [21] was used. The (^{3}He,t) B(GT) values for each mass A system were

TABLE V. List of γ-ray energies and intensities obtained in add-back mode for the decay of ^{46}Cr to ^{46}V.

Energy (keV)	Counts	$I(\gamma)$
915.0 (1)	2437 (121)	28.45 (172)
993.2 (1)	82116 (313)	1000.00 (3521)
1432.5 (1)	16332 (165)	242.03 (882)
1544.4 (2)	626 (89)	9.67 (142)
2062.4 (4)	484 (94)	8.83 (174)
2459.8 (1)	5393 (133)	109.26 (468)
2466.3 (2)	870 (107)	17.66 (226)
2697.4 (1)	3166 (101)	67.90 (321)
2977.8 (1)	7483 (121)	170.77 (658)
3867.6 (4)	235 (46)	6.39 (126)

TABLE VI. List of γ-ray energies and intensities obtained in add-back mode for the decay of ^{42}Ti to ^{42}Sc.

Energy (keV)	Counts	$I(\gamma)$
611.0 (1)	66867 (272)	1000.00 (3523)
1888.4 (2)	272 (37)	7.34 (103)

taken from $A = 54$, Refs. [3,46]; $A = 50$, Ref. [4,46]; $A = 46$, Ref. [5,46]; and $A = 42$, Ref. [6,46]. The Q_β values for the $A = 54$, 50, 46, and 42 systems were taken from Ref. [9].

The comparison between the β-decay B(GT) values and the newly renormalized (^{3}He,t) B(GT) values can be seen in Tables VII–X and in Fig. 18. The uncertainties include the statistical uncertainties as well as the error in the ($T_{1/2}$) and in the Q_β values.

As mentioned, β-decay experiments are limited by the energy window accessible in the decay. On top of that the observation of levels at high excitation energy is difficult because of the combined effect of the Fermi function (f) and the decrease in γ detection efficiency (ϵ^γ) of the Ge detectors or the decay by protons at energies about 1 MeV above the proton binding energy. To take the two first effects into account, we introduce the sensitivity limit defined by

$$\text{Sensitivity limit} = \frac{1}{f \times \epsilon^\gamma}, \quad (6)$$

and it is shown by dots in Fig. 18 (for energies below the expected decay by protons). The resulting curves have been adjusted to the smallest peaks which could be identified in our spectra.

The first thing to notice is that in our experiments we observe all of the states that were observed in the CE reactions [except for the small peak observed at 2790 keV in the ^{50}Cr(^{3}He,t)^{50}Mn reaction]. We did not observe any 1^+ level

TABLE VII. Comparison of B(GT) values obtained in the β decay of ^{54}Ni (present experiment) and the ^{54}Fe(^{3}He,t)^{54}Cr charge-exchange reaction.

β decay[a]		(^{3}He,t)[b]	
Energy (keV)	B(GT)	Energy (keV)	B(GT)
936.7	0.549(39)	936	0.475(14)
2424.6	0.014(2)	2424	0.015(1)
3376.1	0.081(9)	3374	0.076(2)
3889.6	0.080(11)	3892	0.099(3)
4293.4	0.040(17)	4298	0.022(1)
4323.0	0.096(31)		
4543.8	0.105(20)	4546	0.142(4)
4822.8	0.060(13)	4825	0.097(3)
5202.4	0.057(20)	5221	0.014(1)
		5470	0.013(1)
		5762	0.013(1)
		5857	0.011(1)
		5917	0.140(4)

[a]Present work.
[b]From Ref. [3], but renormalized using the present $T_{1/2}$ value; see text.

TABLE VIII. Comparison of B(GT) values obtained in the β decay of ^{50}Fe (present experiment) and the ^{50}Cr(^{3}He,t)^{50}Mn charge-exchange reaction.

β decay[a]		(^{3}He,t)[b]	
Energy (keV)	B(GT)	Energy (keV)	B(GT)
651.0	0.589(45)	652	0.568(16)
2403.8	0.167(15)	2411	0.171(5)
2684.2	0.106(11)	2694	0.123(4)
		2790	0.032(1)
3380.0	0.280(31)	3392	0.400(12)
3643.4	0.069(15)	3654	0.163(5)
4012.7	0.034(16)	4028	0.076(2)
4315.7	0.099(38)	4333	0.119(3)
		4584	0.028(1)
		5011	0.017(1)
		5048	0.035(1)
		5226	0.064(2)
		5389	0.015(1)
		5545	0.048(1)

[a]Present work.
[b]From Refs. [4,46], but renormalized using the present $T_{1/2}$ value; see text.

in the β decay which was not observed in CE except for the possible candidate level at 4323.0-keV excitation energy in ^{54}Co where we have significant doubts about the provenance of the corresponding transition. We note that the resolved doublet at 2459.8 and 2466.3 keV in the β decay of ^{46}Cr appears as a single peak in the (^{3}He,t) spectrum. In general we can say that

TABLE IX. Comparison of B(GT) values obtained in the β decay of ^{46}Cr (present experiment) and the ^{46}Ti(^{3}He,t)^{46}V charge-exchange reaction.

β decay[a]		(^{3}He,t)[b]	
Energy (keV)	B(GT)	Energy (keV)	B(GT)
993.2	0.473(33)	994	0.441(13)
1432.5	0.167(12)	1433	0.146(4)
2459.8	0.211(16)	2461	0.241(7)
2466.3	0.053(6)		
2697.4	0.172(14)	2699	0.244(7)
2977.8	0.640(48)	2978	0.744(22)
		3533	0.025(1)
		3610	0.031(1)
3867.6	0.082(17)	3870	0.139(4)
		4051	0.056(2)
		4325	0.045(1)
		4378	0.036(1)
		4895	0.019(1)
		5544	0.013(1)
		5684	0.027(1)
		5717	0.012(1)

[a]Present work.
[b]From Refs. [5,46], but renormalized using the present $T_{1/2}$ value; see text.

TABLE X. Comparison of B(GT) values obtained in the β decay of ^{42}Ti (present experiment) and the ^{42}Ca(^{3}He,t)^{42}Sc charge-exchange reaction.

β decay[a]		(^{3}He,t)[b]	
Energy (keV)	B(GT)	Energy (keV)	B(GT)
611.0	2.313(148)	611	2.075(60)
1888.4	0.059(9)	1886	0.080(2)
		3688	0.142(4)

[a]Present work.
[b]From Refs. [6,46], but renormalized using the present $T_{1/2}$ value; see text.

isospin symmetry works to a reasonable extent and that one can indeed study GT transitions using the strong interaction for those states which are not accessible in β decay. It also tells us that the "merged analysis" works well for the first excited states, i.e., the ones that contribute the most to the ($T_{1/2}$). However, if we take a closer look at this comparison, and at the higher excited states in particular, we observed some differences. They amount to up to 50% in some cases (see Table VII).

Possible sources of these differences are discussed below. They fall into three categories, namely (i) possible systematic errors in the determination of the B(GT) values in β-decay, (ii) possible differences arising from the use of the CE reactions to extract relative B(GT) values, and (iii) differences originating from the fact that the initial states involved in the β decay and in the CE reactions are not identical. We discuss each of the possible effects below:

(i) First one might consider the possibility of systematic errors in calibrating the efficiency of the γ array. However, as described earlier, we devoted considerable effort to establishing the efficiency curve and there were a number of internal cross-checks which established its soundness and reliability. It is also possible that the observed differences have their origin in the so-called Pandemonium effect in β decay [47]. In essence, it is possible that we underestimate the β feeding to the 1^+ states because the de-excitation of the states can be fragmented into a number of parallel cascades, some of which may not be detected, or overestimate them because we fail to detect gamma feeding to the 1^+ states from levels lying above. However, in the cases studied here this is unlikely because all of the excited states observed decay in the same way, i.e., mainly to the ground state as expected if they are $T = 0$ states as explained in Ref. [40]. A related problem is the fact that there are levels above our sensitivity limit which will most probably decay to the ground state and will produce an "apparently higher" ground-state–to–ground-state feeding. Based on the CE reaction data we estimate that the feeding to states below our sensitivity limit will be in the worst case of ^{54}Ni decay less than 2% and

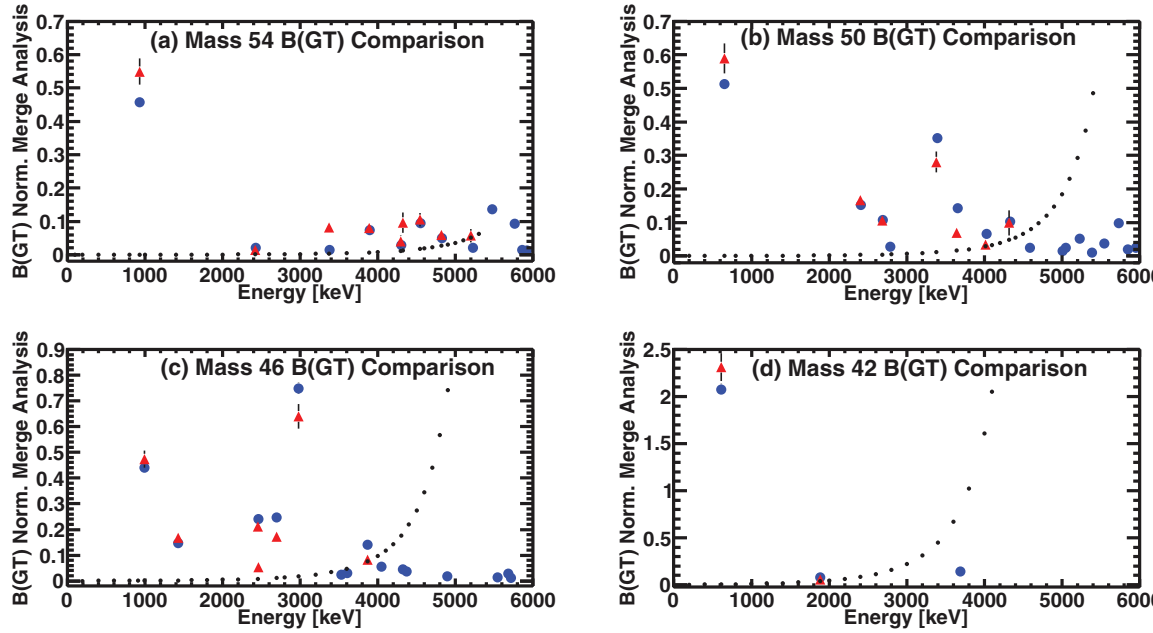

FIG. 18. (Color online) Comparison of B(GT) values obtained in the present analysis (solid red triangles) and those from the (^{3}He,t), CE reactions (solid blue circles) as a function of excitation energy in the daughter nucleus. To derive the absolute B(GT) values from the CE reaction data, the "merged analysis" was used (see text). The dots show the sensitivity limit in the present experiment; for masses 54 and 50 the limit stops at the energy where proton decay is expected to dominate (see text).

will be dominated by proton decay. Consequently, the effect on the ground-state feeding and on the estimated B(GT) values is negligible.

(ii) Turning to the CE reactions it is clear that two-step processes could change the cross section for particular states. However, at an energy of ~140 MeV per nucleon it is generally accepted that such effects should be small. Another difference between β decay and CE is that the latter is peripheral and therefore sensitive to the part of the radial wave function close to the nuclear surface. However, in the cases studied here, we are dealing with valence nucleons in the $f_{7/2}$ or $f_{5/2}$ orbitals, where such differences are small. Larger differences might be anticipated when the next orbital, the $p_{3/2}$, is involved, i.e., in the $A = 58$ system. A more serious source of concern is the possible tensor contributions to the transition between the parent state and the states in the daughter final nucleus. In β decay only the $\Delta L = 0$ $\sigma\tau$ contribution is allowed ($\Delta L = 0, \Delta S = 1, \Delta T = 1$, and thus $\Delta J = 1$), while in CE reactions the amount of momentum transfer is finite even in measurements at 0° because of the finite negative Q value of the reaction. Hence the noncentral isovector-tensor (Tτ) interaction behaving like $\Delta L = 2$, $\Delta S = 1$, $\Delta T = 1$, and thus $\Delta J = 1$, can contribute. This can modify the cross section of the 1^+ excited states and give an extra contribution to the B(GT) values.

(iii) Finally we are concerned in this article with the comparison of two initial states that are mirror states with opposite values of T_z and in principle the same isospin T. If isospin is a good quantum number this would mean that the two states are identical. However, we know that the nuclear Hamiltonian is not charge independent and thus we are not dealing with initial states of pure isospin. The long-range Coulomb force is the most obvious source of the charge dependence effects but the short-range nuclear force is also charge dependent and there is also a charge-dependent spin-orbit component in the nuclear potential because the nucleons have different magnetic moments and charges; see, for example, Ref. [48]. All of these effects lead to isospin mixing of the nuclear states. Ignoring the details of the charge dependence of the Hamiltonian one might expect that (a) the radial wave function of the $T_z = -1$, 0^+ ground state will be more extended than its mirror counterpart because of the repulsion of the extra two protons, and (b) both states will have a dominant $T = 1$ component but might have different admixtures of $T = 2$ isospin in their wave functions. This implies that the transitions to the common $T_z = 0$ final nucleus might differ and thus contribute to the differences in B(GT) that we observe.

The last two points, namely, the possible tensor contributions and different amount of isospin mixing in the parent states, might be possible to calculate theoretically. We hope this paper will stimulate such an effort. Here we provide the experimental approach which can be used to test such calculations in the future.

Finally, to have a full picture of the B(GT) strength as a function of the excitation energy using the information from both experiments it is convenient to look at the accumulated

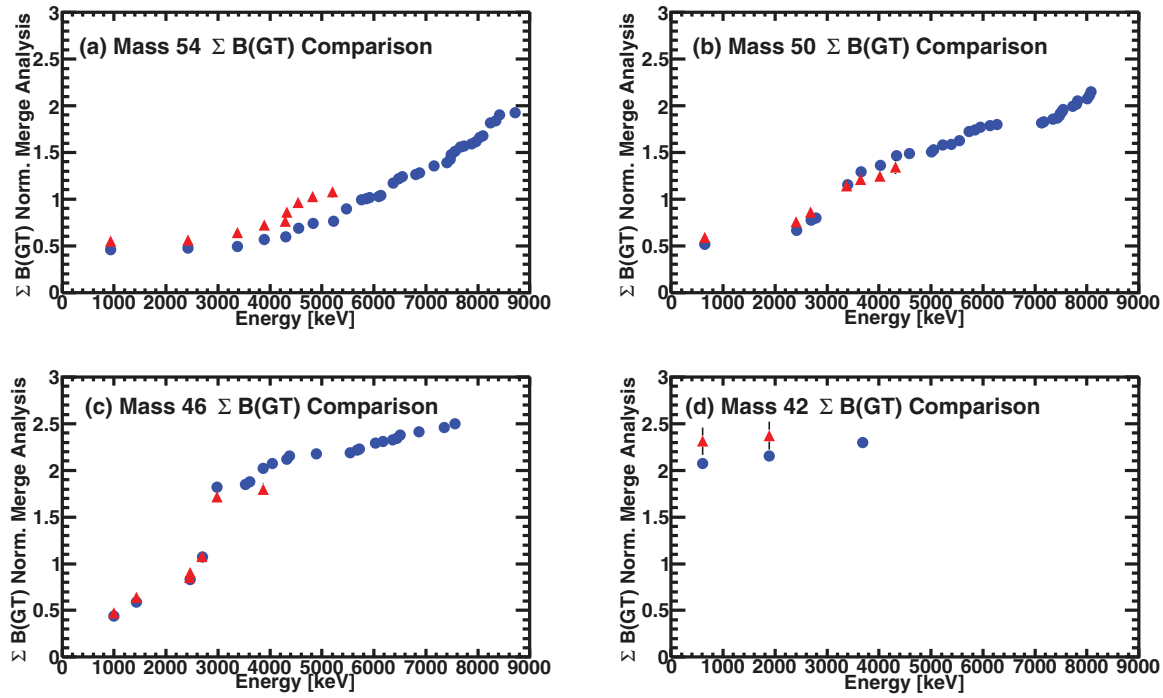

FIG. 19. (Color online) Comparison of accumulated B(GT) values obtained in the present analysis (solid red triangles) and those from the (^{3}He,t), CE reactions (solid blue circles) as a function of excitation energy in the daughter nucleus. To derive the absolute accumulated B(GT) values from the data of CE reactions, the "merged analysis" was used (see text).

strength shown in Fig. 19, where small differences from weak peaks are smoothed out. It is also appropriate because this kind of presentation is often used to compare theory and experiment. If we look at the energy range where data exist for both kinds of experiments, we can see that the results agree very well. On the other hand there are important contributions to the B(GT) inside the Q_β window but below our sensitivity limit in beta decay which today can be extracted only from the CE data. This is clear proof that the "merged analysis" is a very useful tool if we want to discuss the B(GT) distribution in the full Q_β window.

V. SUMMARY AND CONCLUSIONS

In this work we have studied the β decay of the $T_z = -1$ $f_{7/2}$ nuclei ^{54}Ni, ^{50}Fe, ^{46}Cr, and ^{42}Ti, produced in fragmentation reactions at GSI. We have compared them with measurements of the corresponding $T_z = +1$ to $T_z = 0$ CE reactions carried out at RCNP-Osaka. We wanted to test whether these two processes are the same and, if not, how they might differ. This is an interesting problem in itself but also because this idea is used in the so-called "merged analysis" [4] in which one uses the ($T_{1/2}$) value and the Q_β of the β decay to normalize the relative B(GT) values from the CE in the mirror nucleus to obtain a full picture of the B(GT) distribution as a function of excitation energy inside the Q_β window and even beyond. From all possible cases to test this idea the $T = 1$ triplet is the simplest because we start with two mirror initial states but we end up in the same final nucleus. In other words, the possible differences in nuclear structure between the parent-daughter mirror pairs are minimized in this case. We wanted to study several cases and for each case several transitions to make this comparison meaningful.

Our experiments were timely because of the installation of the Ge RISING array at the GSI Fragment Separator, and the high resolution studies of the CE reaction now possible at RCNP-Osaka. Our results represent a significant step forward because up to now it had only been possible to observe β decays to the first excited 1^+ state for three of the four cases studied. The greatly improved decay schemes include the β feeding to the ground state and improved values for the parent ($T_{1/2}$).

The results obtained allowed us to make the comparison of the B(GT) values derived from the β decay, including a sensitivity limit, with the results of the CE studies normalized using the merged analysis. The B(GT) values extracted by the two methods are very similar for the strong transitions that dominate the ($T_{1/2}$). Moreover, all the transitions observed in the CE process and inside our sensitivity limit are also observed in the β-decay experiments. When looking in more detail, however, one finds that there are some differences for the weak transitions. We have considered the possible origins of the differences. We concluded that the most probable reasons are, that the differences lie in the possible tensor contributions in the CE process and/or that the wave functions of the initial parent states may be different for a variety of reasons. To disentangle these two effects one needs further theoretical input, and we hope this work will serve to stimulate an effort in this direction. It is also important to measure other cases with larger T_z and mass. With this idea in mind we have launched and performed a series of experiments at GANIL [49,50].

We have also looked at the accumulated B(GT) as a function of excitation energy in the daughter nucleus; we can see that both probes give very similar results at energies where the beta decay experiment has enough sensitivity, however, looking at the CE experiments, there is some sizable B(GT) strength beyond this point and still inside the Q_β window.

We conclude that the merged analysis can be used to deduce information on the B(GT) strength expected in β decay for those cases where the knowledge of the β decay is very limited, for instance, if we only know the ($T_{1/2}$) and the Q_β value, but also to extract information on how much of the transition strength is expected above the sensitivity limit of our experiments.

Our measurements also add to the information on *superallowed* Fermi transitions between $T_z = -1$ and $T_z = 0$ nuclei which are important for testing the unitarity of the CKM matrix. They extend the systematics on such transitions, carefully collected and analyzed at regular intervals by Hardy and Towner, [7] to higher masses.

ACKNOWLEDGMENTS

The authors would like to thank the GSI accelerator crew and the complete RISING group for their support. This work was partially supported by MICINN-Spain (Grants No. FPA200806419-C02-01 and No. FPA2011-24553), MEXT-Japan (Grants No. 18540270 and No. 22540310), STFC-UK (Grant No. ST/F012012/1), and EC EURONS (Grant No. 506065). B.R. and Y.F. acknowledge the support of the Japan-Spain collaboration program by JSPS and CSIC. R.H. and D.R. acknowledge the support of the Swedish Research Council.

[1] Y. Fujita, B. Rubio, and W. Gelletly, Prog. Part. Nucl. Phys. **66**, 549 (2011), and references therein.
[2] [http://www.fair-center.eu/public/experiment-program/nustar-physics.html].
[3] T. Adachi *et al.*, Phys. Rev. C **85**, 024308 (2012).
[4] Y. Fujita *et al.*, Phys. Rev. Lett. **95**, 212501 (2005).
[5] T. Adachi *et al.*, Phys. Rev. C **73**, 024311 (2006).
[6] T. Adachi *et al.*, Nucl. Phys. A **788**, 70 (2007).
[7] J. C. Hardy and I. S. Towner, Phys. Rev. C **79**, 055502 (2009).
[8] J. C. Hardy and I. S. Towner, Nucl. Phys. News. **16**, 11 (2006).
[9] M. Wang *et al.*, Chin. Phys. C **36**, 1603 (2012).
[10] M. Steiner *et al.*, Nucl. Instrum. Methods Phys. Res. A **312**, 420 (1992).
[11] K.-H. Schmidt *et al.*, Nucl. Instrum. Methods Phys. Res. A **260**, 287 (1987).
[12] H. Geissel *et al.*, Nucl. Instrum. Methods Phys. Res. B **70**, 286 (1992).
[13] R. Kumar *et al.*, Nucl. Instrum. Methods Phys. Res. A **598**, 754 (2009).
[14] S. Pietri *et al.*, Nucl. Instrum. Methods Phys. Res. B **261**, 1079 (2007).
[15] J. Eberth *et al.*, Nucl. Instrum. Methods Phys. Res. A **369**, 135 (1996).
[16] Z. Hu *et al.*, Nucl. Instrm. Methods Phys. Res. A **419**, 121 (1998).
[17] I. Reusen *et al.*, Phys. Rev. C **59**, 2416 (1999).
[18] J. Su *et al.*, Phys. Rev. C **87**, 024312 (2013).
[19] V. T. Koslowsky *et al.*, Nucl. Phys. A **624**, 293 (1997).
[20] T. K. Onishi *et al.*, Phys. Rev. C **72**, 024308 (2005).
[21] T. Kurtukian Nieto *et al.*, Phys. Rev. C **80**, 035502 (2009).
[22] F. Molina, Ph.D thesis, University of Valencia, Valencia, Spain, 2011. [http://digital.csic.es/handle/10261/41939].
[23] Monte Carlo simulation toolkit GEANT4 [http://geant4.cern.ch/].
[24] J. A. Cameron and B. Singh, Nucl. Data Sheets **94**, 429 (2001).
[25] J. Chen, B. Singh, and J. A. Cameron, Nucl. Data Sheets **112**, 2357 (2011).
[26] J. N. Black *et al.*, Phys. Rev. C **11**, 939 (1975).
[27] S. Raman *et al.*, Nucl. Phys. A **184**, 138 (1972).
[28] E. Hagberg *et al.*, Nucl. Phys. A **613**, 183 (1997).
[29] J. Honkanen *et al.*, Nucl. Phys. A **496**, 462 (1989).
[30] D. Rudolph *et al.*, Phys. Rev. C **78**, 021301(R) (2008).
[31] R. P. Yaffe and R. A. Meyer, Phys. Rev. C **16**, 1581 (1977).
[32] S. V. Jackson *et al.*, Phys. Rev. C **12**, 2094 (1975).
[33] T. Sekine *et al.*, Nucl. Phys. A **467**, 93 (1989).
[34] G. Coleman and R. A. Meyer, Phys. Rev. C **13**, 847 (1976).
[35] J. L. Uzureau *et al.*, Phys. Lett. B **331**, 280 (1994).
[36] J. C. Hardy and I. S. Towner, Rep. Prog. Phys. **73**, 046301 (2010).
[37] A. Gallmann *et al.*, Phys. Rev. **186**, 1160 (1969).
[38] F. M. Mann *et al.*, Nucl. Phys. A **258**, 341 (1976).
[39] J. Honkanen, J. Aysto, M. Kortelahti, K. Eskola, and A. Hautojarvi, JYFL (Jyväskylä Finland) Annual Report **1980**, 28 (1980).
[40] G. Morpurgo, Nuovo Cimento **12**, 60 (1954).
[41] T. N. Taddeucci *et al.*, Nucl. Phys. A **469**, 125 (1987).
[42] W. G. Love, K. Nakayama, and M. A. Franey, Phys. Rev. Lett. **59**, 1401 (1987).
[43] Y. Fujita *et al.*, Phys. Rev. C **88**, 014308 (2013).
[44] Y. Fujita *et al.*, Nucl. Instrum. Methods Phys. Res. B **126**, 274 (1997), and references therein.
[45] H. Fujita *et al.*, Nucl. Instrum. Methods Phys. Res. A **484**, 17 (2002).
[46] T. Adachi, Ph.D thesis, Osaka University, Osaka, Japan, 2007.
[47] J. C. Hardy *et al.*, Phys. Lett. B **71**, 307 (1977).
[48] R. J. Blin-Stoyle in *Isospin in Nuclear Physics*, edited by D. F. Wilkinson (North Holland, Amsterdam, 1969).
[49] B. Rubio *et al.*, Nucl. Data Sheets **120**, 37 (2014).
[50] S. E. A. Orrigo *et al.*, Phys. Rev. Lett. **112**, 222501 (2014).